



RESEARCH ARTICLE OPEN ACCESS

Where Do Core Thalamocortical Axons Terminate in Mammalian Neocortex When There Is No Cytoarchitecturally Distinct Layer 4?

Adhil Bhagwandin¹ | Zoltán Molnár²  | Mads F. Bertelsen³ | Karl Æ. Karlsson⁴ | Abdulaziz N. Alagaili⁵ | Nigel C. Bennett⁶ | Patrick R. Hof⁷ | Consolate Kaswera-Kyamakya⁸ | Emmanuel Gilissen^{9,10} | Jaikishan Jayakumar^{11,12} | Paul R. Manger¹ 

¹School of Anatomical Sciences, Faculty of Health Sciences, University of the Witwatersrand, Johannesburg, Republic of South Africa | ²Department of Physiology, Anatomy and Genetics, Sherrington Building, University of Oxford, Oxford, UK | ³Centre for Zoo and Wild Animal Health, Copenhagen Zoo, Frederiksberg, Denmark | ⁴Biomedical Engineering, Reykjavik University, Reykjavik, Iceland | ⁵Department of Zoology, King Saud University, Riyadh, Saudi Arabia | ⁶South African Research Chair of Mammal Behavioural Ecology and Physiology, University of Pretoria, Pretoria, South Africa | ⁷Nash Family Department of Neuroscience, Center for Discovery and Innovation, and Friedman Brain Institute, Icahn School of Medicine at Mount Sinai, New York, New York, USA | ⁸Faculté des Sciences, University of Kisangani, Kisangani, People's Republic of Congo | ⁹Department of African Zoology, Royal Museum for Central Africa, Tervuren, Belgium | ¹⁰Laboratory of Histology and Neuropathology, Université Libre de Bruxelles, Brussels, Belgium | ¹¹Sudha Gopalakrishnan Brain Centre, Indian Institute of Technology Madras, Chennai, India | ¹²Center for Computational Brain Research, Indian Institute of Technology Madras, Chennai, India

Correspondence: Paul Manger (Paul.Manger@wits.ac.za)

Received: 15 March 2024 | **Revised:** 20 May 2024 | **Accepted:** 7 June 2024

Guest Editor: Kathleen Rockland

Funding: This work was supported by funding from the National Research Foundation of South Africa (A.B., P.R.M.), a Royal Society International Exchanges award (P.R.M. and Z.M.), Researchers Supporting Project (RSPD2024R602), King Saud University, Riyadh, Saudi Arabia (A.A.), and the Belgian cooperation service at the Royal Museum for Central Africa (E.G.).

Keywords: cortical evolution | cortical layer IV | cortical layers | cortical processing | RRID-AB_10000321 | RRID-AB_10000340 | RRID-AB_10000343 | RRID-AB_2187552 | RRID-AB_509997 | skin-brain axis

ABSTRACT

Although the mammalian cerebral cortex is most often described as a hexalaminar structure, there are cortical areas (primary motor cortex) and species (elephants, cetaceans, and hippopotami), where a cytoarchitecturally indistinct, or absent, layer 4 is noted. Thalamocortical projections from the core, or first order, thalamic system terminate primarily in layers 4/inner 3. We explored the termination sites of core thalamocortical projections in cortical areas and in species where there is no cytoarchitecturally distinct layer 4 using the immunolocalization of vesicular glutamate transporter 2, a known marker of core thalamocortical axon terminals, in 31 mammal species spanning the eutherian radiation. Several variations from the canonical cortical column outline of layer 4 and core thalamocortical inputs were noted. In shrews/microchiropterans, layer 4 was present, but many core thalamocortical projections terminated in layer 1 in addition to layers 4 and inner 3. In primate primary visual cortex, the sublaminate layer 4 was associated with a specialized core thalamocortical projection pattern. In primate primary motor cortex, no cytoarchitecturally distinct layer 4 was evident and the core thalamocortical projections terminated throughout layer 3. In the African elephant, cetaceans, and river hippopotamus, no cytoarchitecturally distinct layer 4 was observed and core thalamocortical projections terminated primarily in inner layer 3 and less densely in outer layer 3. These findings are

This is an open access article under the terms of the [Creative Commons Attribution-NonCommercial-NoDerivs](https://creativecommons.org/licenses/by-nc-nd/4.0/) License, which permits use and distribution in any medium, provided the original work is properly cited, the use is non-commercial and no modifications or adaptations are made.

© 2024 The Author(s). The *Journal of Comparative Neurology* published by Wiley Periodicals LLC.

1 | Introduction

The mammalian cerebral cortex has been historically divided into six distinct layers, based on cytoarchitectonic patterns, each layer containing a variety of cell types and contributing to specific aspects of neural information processing. The classical view of vertical intracortical processing relates that core thalamocortical axons, which project to almost the entire cortical mantle and transmit the neural information forming the basis of perception, terminate on neurons in layer 4 and deep layer 3 (e.g., Jones 2007; Sherman and Guillery 2002). These neurons then project to the neurons of layers 3 and 2, which in turn project to the neurons of the deeper cortical layers 5 and 6 that take cortically processed information to other regions of the brain (e.g., Douglas and Martin 2004; Gilbert and Wiesel 1979; Jones 2007). Although this view, developed in primary sensory cortical regions, is broadly applicable across mammals, it does not address where thalamocortical axons might terminate, or how intracortical processing may be modified, in cases when there is no cytoarchitecturally distinct layer 4, such as the agranular regions of primate cerebral cortex (e.g., the primary motor cortex), or in species, such as elephants, cetaceans, and hippopotami, whose entire cerebral cortex lacks a cytoarchitecturally distinct layer 4 (Butti et al. 2014; Furutani 2008; Glezer, Jacobs, and Morgane 1988; Hakeem et al. 2009; Jacobs et al. 2011; Major 1879; Manger 2006).

The thalamocortical pathway is not a simple unitary projection, rather it can be divided into a dual projection system: a diffuse thalamic matrix projection (also called higher order thalamic system) that terminates primarily in cortical layers 1 and 2 to modulate cortical arousal, and a focused thalamic core projection (also called the first order thalamic system) that terminates primarily in layer 4 and deep layer 3 that passes information relevant to the contents of experience (Jones 1998; Sherman and Guillery 2002; Travis 2012). Thus, the core thalamic projection plays a central role in cortical processes that lead to the varied behavioral outcomes observed based on perception. This view is based on the concept that all regions of the neocortex in mammals possess a layer 4, but there are regions of the cortex, and species, where layer 4 is architecturally indistinct, or perhaps absent. Hence, we can ask: (1) Where do the core, or first order, thalamocortical axonal projections primarily terminate when there is no architecturally distinct, or absent, layer 4? and (2) what might the consequences of the observed variances be? A simple prediction would be that the core thalamocortical axonal projections will most likely primarily terminate in inner layer 3, perhaps with some spread into outer layer 3 (e.g., in cetaceans, Revishchin and Garey 1991); however, it has also been proposed that in cetaceans (Glezer et al. 1988; Graic et al. 2024), the core thalamocortical axonal projections will be mixed with the diffuse matrix, or higher order, thalamocortical axonal projections and terminate in layers 1 and 2 of the cerebral cortex.

In order to determine the laminar terminations of the core thalamocortical axonal projections in cortical regions and cortices where there is no cytoarchitecturally distinct layer 4, we used immunohistochemical staining for vesicular glutamate transporter 2 (vGlut2), a transporter that has been demonstrated to be localized within the axonal terminals of core, or first order, thalamocortical axons across a range of mammalian species (Balam and Kaas 2014; Balam, Hackett, and Kaas 2013, 2015; Bryant et al. 2012; Graziano et al. 2008; Hackett and de la Mothe 2009; Kaneko, Fujiyama, and Hioki 2002; Marion et al. 2013; Nahmani and Erisir 2005; Wong and Kaas 2008, 2009). We specifically examined regions of the cerebral cortex from various eutherian mammals that could be classified as (1) *typical*, in that they possessed six cortical layers with a cytoarchitecturally distinct layer 4 that presented with no sublamination (e.g., occipital cortex); (2) *specialized*, in that the cytoarchitecturally distinct layer 4 was sublaminated (e.g., primate primary visual cortex); and (3) *atypical*, in that they lacked a cytoarchitecturally distinct layer 4 (e.g., primate primary motor cortex, and occipital and temporal cortices in elephant, cetaceans, and hippopotamus).

2 | Materials and Methods

2.1 | Specimens

All animals used in the current study were adults of the respective species (being of reproductive age but not senescent), although precise ages and sex were not noted. The animals were treated and used according to the guidelines of the University of Witwatersrand Animal Ethics Committee (AESC No. 2012/53/01) that correspond to those of the NIH for care and use of animals in scientific experimentation. The brains were obtained after the animals were euthanized with sodium pentobarbital (i.p.) in line with management decisions independent of the current study (e.g., Bertelsen 2018), or for use in other unrelated studies (Manger et al. 2009). For smaller mammals, once euthanized, the right atrium was opened, and the left ventricle cannulated to allow whole-body perfusion with an initial rinse of 0.9% saline solution at a temperature of 4°C, followed by 4% paraformaldehyde in 0.1 M phosphate buffer (PB) at 4°C. For larger mammals, once euthanized the heads were removed, and the cranial vasculature perfused with an initial rinse of 0.9% saline solution at a temperature of 4°C, followed by 4% paraformaldehyde in 0.1 M PB at 4°C (e.g., Manger et al. 2009). The brains, which showed no signs of neuropathology, were removed from the skull and postfixed in 4% paraformaldehyde in 0.1 M PB (24 h at 4°C), allowed to equilibrate in 30% sucrose in 0.1 M PB and then stored in an antifreeze solution at -20°C until use (Manger et al. 2009). A complete list of the species examined in the current study is provided in Table 1, and for each species, tissue blocks from two individuals were processed.

TABLE 1 | Species investigated, presence/sublamination/absence of an architecturally distinct layer 4, and the layers with the densest vGlut2 immunopositive terminals.

Species name	Common name	Tissue location	Layer 4	Highest vGlut2 laminar terminal densities
Afrotheria				
<i>Loxodonta africana</i>	African bush elephant	Occipital	Absent	3o, 3i
<i>Procavia capensis</i>	Rock hyrax	Occipital	Present	3, 4, 6
Erinaceidae				
<i>Paraechinus aethiopicus</i>	Desert hedgehog	Occipital	Present	3, 4, 6
<i>Atelerix frontalis</i>	Southern African hedgehog	Occipital	Present	3, 4, 6
Soricidae				
<i>Sylvisorex ollula</i>	Greater forest shrew	Occipital	Present	1, 2, 3, 4, 6
Microchiroptera				
<i>Hipposideros fuliginosus</i>	Sooty roundleaf bat	Occipital	Present	1, 2, 3, 4, 6
<i>Hipposideros commersoni</i>	Commerson's leaf-nosed bat	Occipital	Present	1, 2, 3, 4, 6
<i>Coleura afra</i>	African sheath-tailed bat	Occipital	Present	1, 2, 3, 4, 6
<i>Chaerephon pumilus</i>	Little free-tailed bat	Occipital	Present	1, 2, 3, 4, 6
<i>Miniopterus schreibersii</i>	Common bent-wing bat	Occipital	Present	1, 2, 3, 4, 6
<i>Asellia tridens</i>	Trident leaf-nosed bat	Occipital	Present	1, 2, 3, 4, 6
<i>Cardioderma cor</i>	Heart-nosed bat	Occipital	Present	1, 2, 3, 4, 6
<i>Nycteris macrotis</i>	Large-eared slit-faced bat	Occipital	Present	1, 2, 3, 4, 6
Cetartiodactyla				
<i>Giraffa camelopardalis</i>	Giraffe	Occipital	Present	3, 4, 6
<i>Damaliscus pygargus</i>	Blesbok	Occipital	Present	3, 4, 6
<i>Phocoena phocoena</i>	Harbor porpoise	Occipital	Absent	3o, 3i
<i>Phocoena phocoena</i>	Harbor porpoise	Temporal	Absent	3o, 3i
<i>Balaenoptera acutorostrata</i>	Minke whale	Occipital	Absent	3o, 3i
<i>Balaenoptera acutorostrata</i>	Minke whale	Temporal	Absent	3o, 3i
<i>Hippopotamus amphibius</i>	River hippopotamus	Occipital	Absent	3o, 3i
<i>Hippopotamus amphibius</i>	River hippopotamus	Temporal	Absent	3o, 3i
<i>Sus scrofa</i>	Domestic pig	Occipital	Present	3, 4, 6
<i>Camelus dromedarius</i>	Dromedary camel	Occipital	Present	3, 4, 6
Scandentia				
<i>Tupaia belangeri</i>	Northern tree shrew	Occipital	Present	3, 4, 6
Megachiropterans				
<i>Epomops franqueti</i>	Franquet's epauletted fruit bat	Occipital	Present	3, 4, 6
<i>Megaloglossus woermanni</i>	Woermann's fruit bat	Occipital	Present	3, 4, 6
<i>Epomophorus wahlbergi</i>	Wahlberg's epauletted fruit bat	Occipital	Present	3, 4, 6
<i>Hypsignathus monstrosus</i>	Hammer-headed bat	Occipital	Present	3, 4, 6
<i>Rousettus aegyptiacus</i>	Egyptian rousette	Occipital	Present	3, 4, 6
<i>Casinycteris argynnis</i>	Short-palated fruit bat	Occipital	Present	3, 4, 6
Primates				
<i>Lemur catta</i>	Ring-tailed lemur	VI	Sublaminated	3(C), 4A, 4B, 6
<i>Lemur catta</i>	Ring-tailed lemur	3b	Present	3, 4, 6
<i>Lemur catta</i>	Ring-tailed lemur	MI	Absent	3, 6

(Continues)

TABLE 1 | (Continued)

Species name	Common name	Tissue location	Layer 4	Highest vGlut2 laminar terminal densities
<i>Saimiri sciureus</i>	Squirrel monkey	VI	Sublaminated	3Bβ, 4A, 4B, 6
<i>Saimiri sciureus</i>	Squirrel monkey	3b	Present	3, 4, 6
<i>Saimiri sciureus</i>	Squirrel monkey	MI	Absent	3, 6
<i>Chlorocebus pygerythrus</i>	Vervet monkey	VI	Sublaminated	3Bβ, 4A, 4B, 6
<i>Chlorocebus pygerythrus</i>	Vervet monkey	3b	Present	3, 4, 6
<i>Chlorocebus pygerythrus</i>	Vervet monkey	MI	Absent	3, 6
<i>Papio ursinus</i>	Chacma baboon	VI	Sublaminated	3Bβ, 4A, 4B, 6
<i>Papio ursinus</i>	Chacma baboon	3b	Present	3, 4, 6
<i>Papio ursinus</i>	Chacma baboon	MI	Absent	3, 6

Note: 3o—outer sub-lamina of layer 3; 3i—inner sub-lamina of layer 3; 3(C)—inner sublamina of layer 3 in the primary visual cortex of prosimian primates; 3Bβ—specialized sublamina of layer 3 in the primary visual cortex of simian primates; 4A—outer sublayer of layer 4 in the primary visual cortex of primates; 4B—inner sublayer of layer 4 in the primary visual cortex of primates.

2.2 | Sectioning and Immunohistochemical Staining

Blocks of cerebral cortex from the occipital lobe (striate or extrastriate visual cortex) were taken from all specimens. In many of the species examined, the location of primary visual (striate) cortex has not been systematically defined, thus using the term occipital is more appropriate and cautious, but the blocks from the occipital lobe of primates were definitively located in cortical area V1 based on cytoarchitectural comparisons to the previous work (e.g., Balaram and Kaas 2014). The examination of the occipital cortex/V1 across species allowed us to properly contextualize the known specializations of primate V1 vGlut2 immunostaining (Balaram and Kaas 2014) with the other species examined, that is, we could reveal how a specialized layer 4 may affect thalamocortical input. In the two cetacean species, river hippopotamus and the African elephant additional blocks were taken from the temporal lobe (presumably primary auditory cortex). The occipital and temporal blocks taken for examination in the two cetacean species, river hippopotamus and African elephant, all of which are reported to lack a cytoarchitecturally distinct layer 4, represent regions of the cortex where the primary visual and auditory cortical areas are most likely to be located. This selection of tissue blocks allowed us to contextualize what variations may occur in the thalamocortical input revealed by vGlut2 immunostaining when no cytoarchitecturally distinct layer 4 is present. We specifically targeted the presumed primary sensory areas in these species as these should be in receipt of high-density thalamocortical inputs. In the four species of primates studied, additional blocks of tissue that encompassed the somatomotor cortex (primary somatosensory, area 3b, and primary motor cortex, area M1, as defined cytoarchitecturally and by location on the rostral and caudal banks of the central sulcus where present) were taken from each specimen. These blocks served two purposes: first, the primary motor cortex reportedly lacks a cytoarchitecturally distinct layer 4 and thus provides additional information regarding the fate of thalamocortical axonal terminations when layer 4 is not present. In addition, the examination of primary somatosensory cortex provides an “internal” control for the primates, as the primary somatosensory

cortex does possess a cytoarchitecturally distinct layer 4, but this layer 4 is not sublaminated as in the primary visual cortex of primates and thus represents the more commonly observed cytoarchitecture of the mammalian cerebral cortex. Thus, in primates, we examined a cortical area with a specialized layer 4 (V1), one that lacks a cytoarchitecturally distinct layer 4 (M1), and one that presents with what can be considered a “typical” layer 4 (area 3b).

The blocks were allowed to equilibrate in 30% sucrose in 0.1 M PB and then frozen in crushed dry ice. The frozen blocks were mounted to an aluminum stage, and 50 μm thick sections, orthogonal to the pial surface, were cut using a sliding microtome. In all species, the sections were stained for Nissl and vGlut2. In primate primary visual cortex, plus occipital cortex in the rock hyrax, and occipital and temporal cortex in the harbor porpoise and river hippopotamus, sections were also stained for parvalbumin (PV). In the African elephant and minke whale, additional sections were stained for myelin, PV, calbindin (CB), calretinin (CR), and non-phosphorylated neurofilament H (NFH, elephant only) to assist in the determination of the presence/absence of layer IV. Sections used for Nissl staining were mounted on 0.5% gelatine-coated glass slides and then cleared in a solution of 1:1 chloroform and 100% alcohol overnight, after which the sections were then stained with 1% cresyl violet. The sections used for myelin staining were refrigerated for 2 weeks in 5% formalin then mounted on 1.0% gelatine-coated slides and stained with a modified silver stain (Gallyas 1979).

The sections used for immunohistochemistry were initially treated for 30 min with an endogenous peroxidase inhibitor (49.2% methanol: 49.2% 0.1 M PB: 1.6% of 30% H₂O₂), followed by three 10 min rinses in 0.1 M PB. Sections were then preincubated for 2 h, at room temperature, in blocking buffer (containing 3% normal goat serum, NGS, for PV, CB, and CR immunostaining, or 3% normal horse serum, NHS, for vGlut2 and NFH immunostaining, plus 2% bovine serum albumin, BSA, and 0.25% Triton X-100 in 0.1 M PB). Thereafter sections were incubated in the primary antibody solution, made up of the appropriate dilution of the primary antibody (see Table 2) in blocking buffer for 48 h

TABLE 2 | Sources and dilution of antibodies used in the current study.

Antibody	Host	Immunogen	Manufacturer	Catalogue No.	Reference	Dilution	RRID
PV	Rabbit	Rat muscle parvalbumin	Swant	PV28	Celio (1990)	1:10000	AB_10000343
CB	Rabbit	Rat recombinant calbindin D-28k	Swant	CB38a	Celio (1990)	1:10000	AB_10000340
CR	Rabbit	Recombinant human calretinin containing a 6-his tag at the N-terminal	Swant	7699/3H	Schwaller et al. (1997)	1:10000	AB_10000321
vGlut2	Mouse	Recombinant protein from rat vesicular glutamate transporter 2	Merck-Millipore	MAB5504	Griffin et al. (2010) and Wong et al. (2008)	1:4000	AB_2187552
SMI-32	Mouse	Non-phosphorylated epitope of neurofilament H from rat hypothalami	Covance	SMI-32R	Sternberger and Sternberger (1983)	1:1000	AB_509997

Abbreviations: CB, calbindin; CR, calretinin; PV, parvalbumin; SMI-32, antibody raised against non-phosphorylated neurofilament H; vGlut2, vesicular glutamate transporter 2.

at 4°C under gentle agitation. The primary antibody incubation was followed by three 10-min rinses in 0.1 M PB, and the sections were then incubated in a secondary antibody solution (containing a 1:1000 dilution of biotinylated anti-rabbit IgG, BA 1000, Vector Labs, for PV, CB, CR immunostaining, or biotinylated anti-mouse IgG, BA2001, Vector Labs, for vGlut2 and NFH immunostaining, in a solution made up of 3% NGS/NHS and 2% BSA in 0.1 M PB) for 2 h at room temperature. This was followed by three 10 min rinses in 0.1 M PB after which the sections were incubated in AB solution (Vector Labs) for 1 h. After three further 10 min rinses in 0.1 M PB, the sections were placed in a solution of 0.05% 3,3'-diaminobenzidine in 0.1 M PB for 5 min (2 mL/section), followed by the addition of 3 µL of 30% H₂O₂ to each 1 mL of solution in which each section was immersed. Chromatic precipitation of the sections was monitored visually under a low-power stereomicroscope. This process was allowed to continue until the background staining of the sections was appropriate for analysis without obscuring any immunoreactive neuronal structures. The precipitation process was stopped by immersing the sections in 0.1 M PB and then rinsing them twice more in 0.1 M PB. To check for nonspecific staining from the immunohistochemistry protocol, we omitted the primary antibody and the secondary antibody in selected sections, which produced no evident staining. The immunohistochemically stained sections were mounted on 0.5% gelatine-coated slides and left to dry overnight. The sections were then dehydrated in graded series of alcohols, cleared in xylene, and cover slipped with DePeX.

2.3 | Qualitative Analysis

All sections were examined with a light microscope at low and high magnifications, and the immunoreactivity in each species was recorded. Digital photomicrographs were captured using an Axiocam 208 color camera mounted to a Zeiss Axioskop microscope (with Zeiss A-Plan 5X/012, Zeiss Plan-NeoFluar 10X/0.30, and Zeiss Plan-NeoFluar 40X/0.75 objectives). No pixelation adjustments or manipulations of the captured images were undertaken, except for the adjustment of contrast, brightness, and levels using Adobe Photoshop on the captured images as a whole.

2.4 | Antibody Characterization and Specificity

The antibodies used and associated details are listed in Table 2.

2.4.1 | Parvalbumin (PV)

To reveal neurons expressing PV, we used the PV28 anti-PV rabbit polyclonal antibody from Swant (PV28, Swant; RRID AB_10000343) at a dilution of 1:5000. The pattern of immunoreactivity in the cerebral cortex was mostly similar across mammals, with PV being expressed in a subset of cortical neurons and their axonal projections (del Campo, Measor, and Razak 2014; Griffen and Maffei 2014; Jones 1998, 2001, 2003; Rubio-Garrido, Perez-De-Manzo, and Clasca 2007).

2.4.2 | Calbindin (CB)

To reveal neurons expressing CB, we used the CB38a anti-CB rabbit polyclonal antibody from Swant (CB38a, Swant; RRID AB_10000340) at a dilution of 1:5000. The pattern of immunoreactivity in the cerebral cortex was mostly similar across mammals, but with specific variances of interest.

2.4.3 | Calretinin (CR)

To reveal neurons expressing CR, we used the 7699/3H anti-CR rabbit polyclonal antibody from Swant (7699/3H, Swant; RRID AB_10000321) at a dilution of 1:5000. The pattern of immunoreactivity in the cerebral cortex was mostly similar across mammals, but with specific variances of interest.

2.4.4 | Vesicular Glutamate Transporter 2 (vGlut2)

The vGlut2 mouse monoclonal antibody was raised against the recombinant vGlut2 protein from the rat (MAB5504; Merck-Millipore; RRID AB_2187552) (Griffin et al. 2010;

Wong et al. 2008). This antibody was used at a dilution of 1:4000. The vGlut2 protein is found in the axonal terminals of core thalamic relay neurons (Balam and Kaas 2014; Balam et al. 2013, 2015; Bryant et al. 2012; Graziano et al. 2008; Hackett and de la Mothe 2009; Kaneko et al. 2002; Marion et al. 2013; Nahmani and Erisir 2005; Wong and Kaas 2008, 2009).

2.4.5 | Neurofilament H (NFH)

The SMI-32 mouse monoclonal IgG1 antibody was produced against the non-phosphorylated epitope of NFH isolated from homogenized rat hypothalami recovered (SMI-32; Covance, Princeton, NJ; RRID AB_509997) (Goldstein, Sternberger, and Sternberger 1987; Sternberger 1986; Sternberger and Sternberger 1983). The antibody reacts with a non-phosphorylated epitope from the 200 kDa neurofilament heavy chain of most mammalian species (Sternberger 1986). This protein is expressed in neuronal cell bodies, dendrites, and some thick axons (Sternberger and Sternberger 1983) and selectively labels the sub-cerebral projecting layer 5 pyramidal neurons in rat and mouse but is not expressed in the layer 5 neurons with callosal projections (Voelker et al. 2004). This antibody was used at a dilution of 1:1000.

3 | Results

Immunohistochemical staining for vGlut2 revealed the presence of axonal terminals in all layers of all cortical areas in all species investigated; however, qualitatively assessed differences in the densities of these terminals, which correspond to layer boundaries, were apparent. These variations were most often, but not always, associated with differences in the appearance of cortical layer 4 (*typical* vs. *specialized* vs. *atypical*, see below for specific definitions used) and allowed us to define six distinct patterns of vGlut2-immunopositive axonal terminal staining in the neocortex of the eutherian mammals investigated in the current study.

3.1 | vGlut2 Axonal Terminal Laminar Densities in Cortices With a Typical Layer 4

We define a *typical* cortical layer 4 as being one where the layer was readily cytoarchitecturally defined, composed of granular cells, and did not exhibit any sublamination. This *typical* layer 4 was identified in the occipital cortex of the rock hyrax, desert hedgehog, Southern African hedgehog, greater forest shrew, eight microchiropteran species, giraffe, blesbok, domestic pig, dromedary camel, northern tree shrews, six megachiropteran species, and the primary somatosensory cortex of four primate species (Table 1). In the species where a *typical* layer 4 was present, vGlut2-immunopositive axonal terminal densities, as assessed qualitatively, were observed to form two distinct patterns.

3.1.1 | Most Commonly Observed vGlut2 Axonal Terminal Laminar Density Pattern

In the occipital cortex of the rock hyrax (Figure 1), desert hedgehog, Southern African hedgehog (Figure 2), giraffe, blesbok, domestic pig, dromedary camel (Figure 3), northern tree

shrew, six megachiropteran species (Figure 4), and the primary somatosensory cortex of four primate species (Figure 5), the qualitatively assessed pattern of vGlut2-immunopositive axonal terminal laminar densities was very similar. In these cortical regions of these species, although vGlut2-immunopositive axonal terminals were observed in all cortical layers, the highest densities were observed in layer 4 (Figures 1–5). The inner half of layer 3 (while not being obviously cytoarchitecturally distinct from the outer half of layer 3) also contained a substantial density of vGlut2-immunopositive axonal terminals (Figures 1–5). A clear, but relatively lower, density of vGlut2-immunopositive axonal terminals was observed in layer 6 (Figures 1–5).

3.1.2 | The Greater Forest Shrew and Microchiropteran vGlut2 Axonal Terminal Laminar Density Pattern

Although the occipital cortex of the greater forest shrew and the eight microchiropteran species studied all exhibited what could be described as a *typical* layer 4, the pattern of vGlut2-immunopositive axonal terminal laminar densities exhibited clear differences compared to the species described above. As with the species described above, the highest densities of vGlut2-immunopositive axonal terminals were observed in layer 4, followed by inner layer 3 and then layer 6 (Figure 2c–h,j–l,n–p,r–t); however, in the greater forest shrew and the eight microchiropteran species, bundles of vGlut2-immunopositive axons were observed to pass through layer 2, with substantial densities of vGlut2-immunopositive axonal terminals being observed in both layers 2 and 1 (Figure 2c–h,j–l,n–p,r–t). Thus, in the greater forest shrew and the eight microchiropterans, almost all cortical layers exhibit moderate to high densities of vGlut2-immunopositive axonal terminals.

3.2 | vGlut2 Axonal Terminal Laminar Densities in Cortices With a Specialized Layer 4

We define a *specialized* cortical layer 4 as being one where the layer was readily cytoarchitecturally defined, composed of granular cells, and exhibited sublamination. This *specialized* layer 4 was identified in the primary visual cortex of the four species of primates studied (Figure 6). In the primate species where a *specialized* layer 4 was present in the primary visual cortex, vGlut2-immunopositive axonal terminal densities, as assessed qualitatively, were observed to form two distinct patterns, one associated with the prosimian studied and the second with the three simians studied.

3.2.1 | vGlut2 Axonal Terminal Laminar Densities in Cortices With a Specialized Layer 4—Prosimian Primary Visual Cortex

In the primary visual cortex of the ring-tailed lemur, vGlut2-immunopositive axonal terminals were observed in all cortical layers. Layer 4B exhibited the greatest density of vGlut2-immunopositive axonal terminals, with layer 4A showing a slight decrease in vGlut2-immunopositive axonal terminal density (Figure 6a,b,o). A moderate density of vGlut2-immunopositive axonal terminals was noted in layer 6 (Figure 6a,b,s). In the ring-tailed lemur, a moderate density of vGlut2-immunopositive

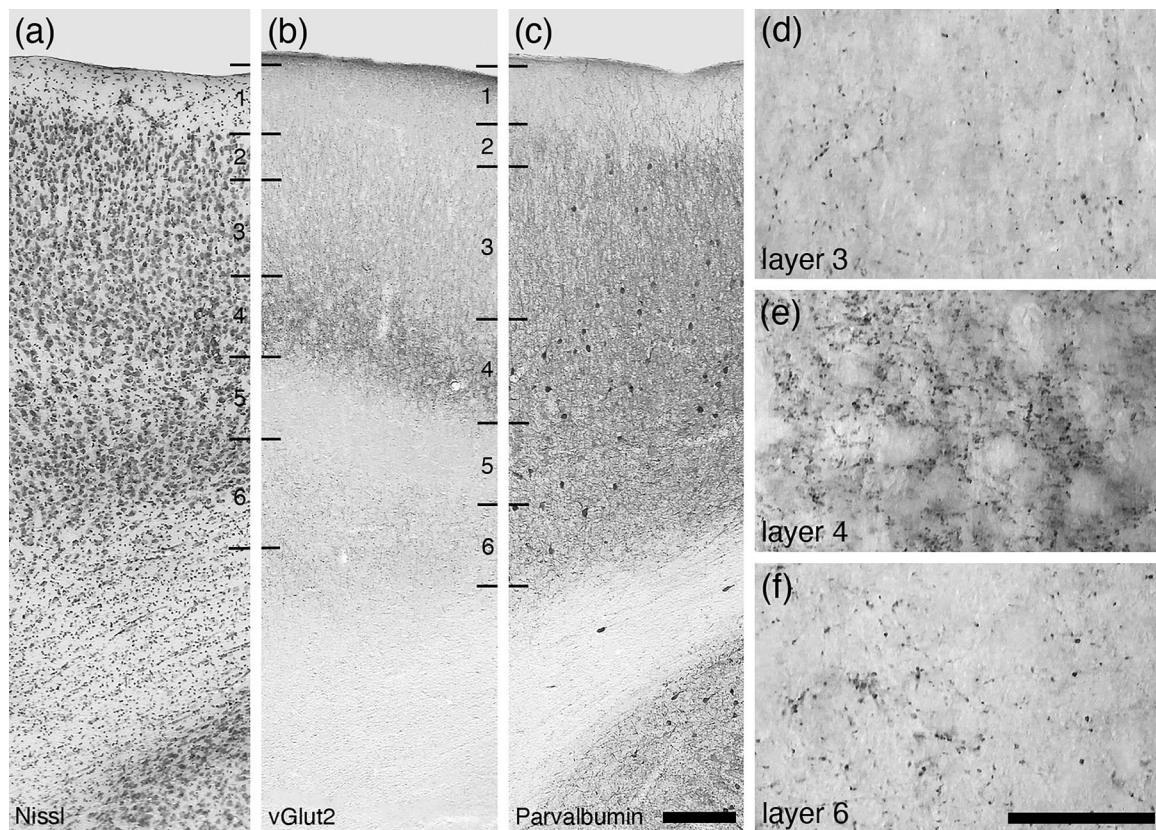


FIGURE 1 | Photomicrographs of Nissl (a), vGlut2 (b, d–f), and PV (c) stained sections through the occipital cortex of the rock hyrax. In all images, the pial surface is to the top of the image. Layer demarcations are indicated by thin horizontal black lines. Although vGlut2-immunopositive axonal terminals were observed in all layers, the most significant terminal densities were observed in layers 3, 4, and 6. Scale bar in (c) = 200 μ m and applies to (a)–(c). Scale bar in (f) = 50 μ m and applies to (d)–(f). vGlut2, vesicular glutamate transporter 2.

axonal terminals was observed in the inner portion of layer 3 (presumably layer 3C; Figure 6a,b,k).

areas (in the same primate brains, see above regarding primary somatosensory cortex) where a *typical* layer 4 is observed.

3.2.2 | vGlut2 Axonal Terminal Laminar Densities in Cortices With a *Specialized* Layer 4—Simian Primary Visual Cortex

In the primary visual cortex of the three simian species (squirrel monkey, vervet monkey, chacma baboon), vGlut2-immunopositive axonal terminals were observed in all cortical layers. Like the ring-tailed lemur, in the simians examined layer 4B exhibited the greatest density of vGlut2-immunopositive axonal terminals, with layer 4A showing a slight decrease in vGlut2-immunopositive axonal terminal density (Figure 6c–j,p–r). A moderate density of vGlut2-immunopositive axonal terminals was noted in layer 6 in all three simians (Figure 6c–j,t–v). In contrast to the ring-tailed lemur, in the simians studied, the vGlut2-immunopositive axonal terminals of layer 3 were located specifically within what is termed layer 3B β and exhibited a moderate-to-high density (Figure 6c–j,l–n). The pattern of vGlut2-immunopositive axonal terminal densities in the primary visual cortex of primates, especially simian primates, where a *specialized*, sublaminate, layer 4 is present, is different from that observed in other mammals and other cortical

3.3 | vGlut2 Axonal Terminal Laminar Densities in Cortices With an *Atypical* Layer 4

We define an *atypical* cortical layer 4 as being one where the layer was not readily cytoarchitecturally defined, and no clear evidence of granular cells was present. Additionally, the cortical depth where layer 4 may have been located is coincident with the cytoarchitecturally defined boundary between layers 3 and 5. This definition does not preclude the possible presence of a cryptic layer 4, for example, the granular cells may be dispersed through other cortical layers, but it does indicate that there is a significant qualitative difference between species classified as having an *atypical* layer 4 when compared to those with either a *typical* or *specialized* layer 4. In the species studied herein, we observed an *atypical* layer 4 in the primary motor cortex of the four primate species studied, and throughout the neocortex of the African elephant, harbor porpoise, minke whale, and river hippopotamus. In these species where an *atypical* layer 4 was noted, vGlut2-immunopositive axonal terminal densities, as assessed qualitatively, were observed to form two distinct patterns.

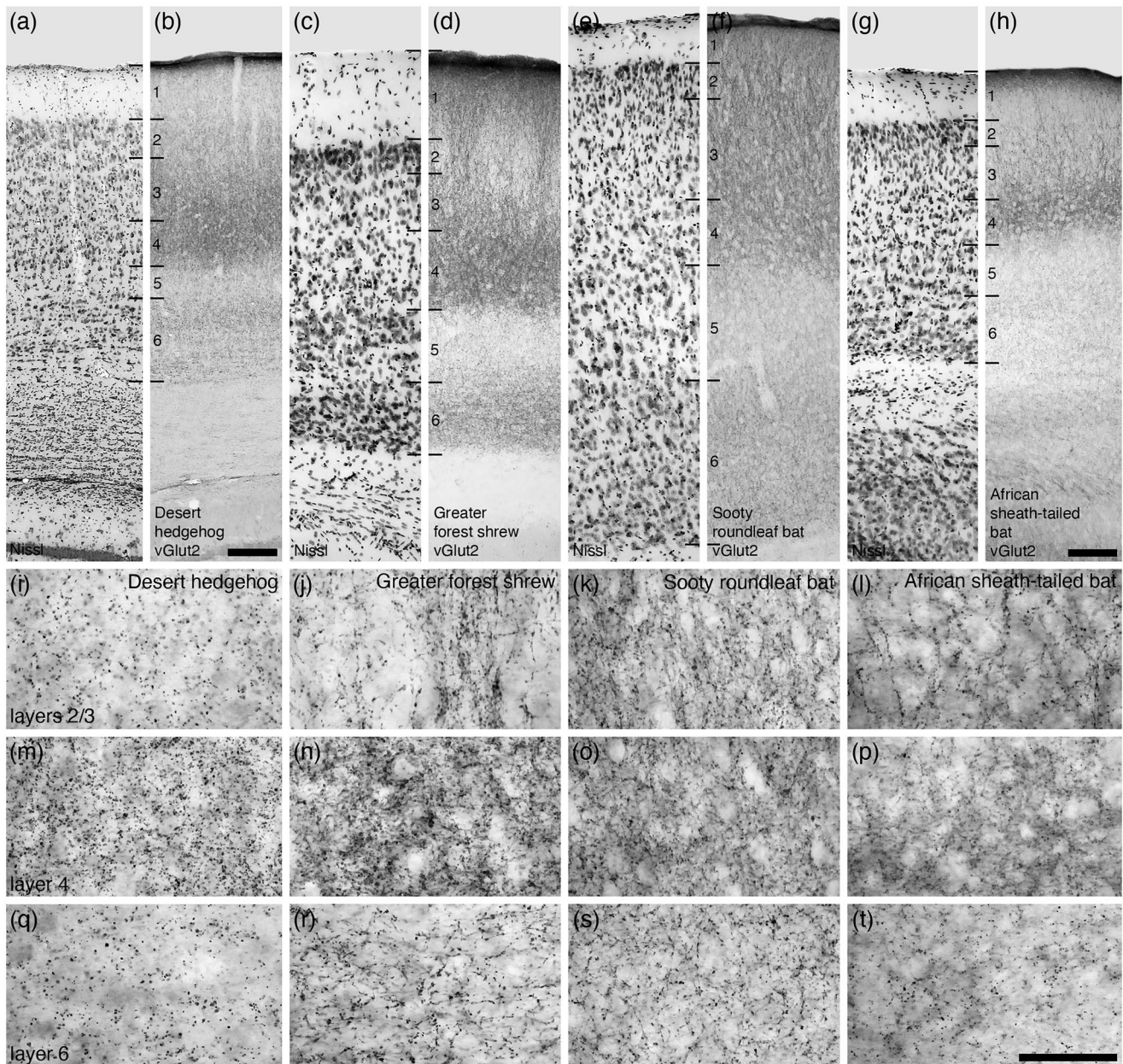


FIGURE 2 | Photomicrographs of Nissl (a, c, e, g) and vGlut2 (b, d, f, h, i–t) stained sections through the occipital cortex of the desert hedgehog (a, b, i, m, q), greater forest shrew (c, d, j, n, r), sooty roundleaf bat (e, f, k, o, s), and African sheath-tailed bat (g, h, l, p, t). In all images, the pial surface is to the top of the image. Layer demarcations are indicated by thin horizontal black lines. Although vGlut2-immunopositive axonal terminals were observed in all layers, the most significant terminal densities were observed in layers 3, 4, and 6. Interestingly, in the shrew and microbats, the vGlut2-immunopositive axons formed fasciculi that extended superficially through layer 2 to densely innervate layer 1, but this was not observed in the desert hedgehog. Scale bar in (b) = 200 μ m and applies to (a) and (b). Scale bar in (h) = 100 μ m and applies to (c)–(h). Scale bar in (t) = 50 μ m and applies to (i)–(t). vGlut2, vesicular glutamate transporter 2.

3.3.1 | vGlut2 Axonal Terminal Laminar Densities in Cortices With an Atypical Layer 4—Primate Primary Motor Cortex

In the primate primary motor cortex, cytoarchitecturally delineated by the presence of Betz cells in layer 5 (Figure 7a,c,e,g), vGlut2-immunopositive axonal terminals were observed in all cortical layers, but the overall density was substantially lower

than observed in other regions of the cerebral cortex of other species (Figure 7b,d,g,f,i–p). Moderate densities of vGlut2-immunopositive axonal terminals were noted throughout layer 3 (Figure 7b,d,f,h,i–l), with lower densities being observed in layer 6 (Figure 7b,d,f,h,m–p). In the squirrel monkey, a low density of soma was vGlut2-immunopositive as shown previously in the chimpanzee and marmoset (Balaram and Kaas 2014).

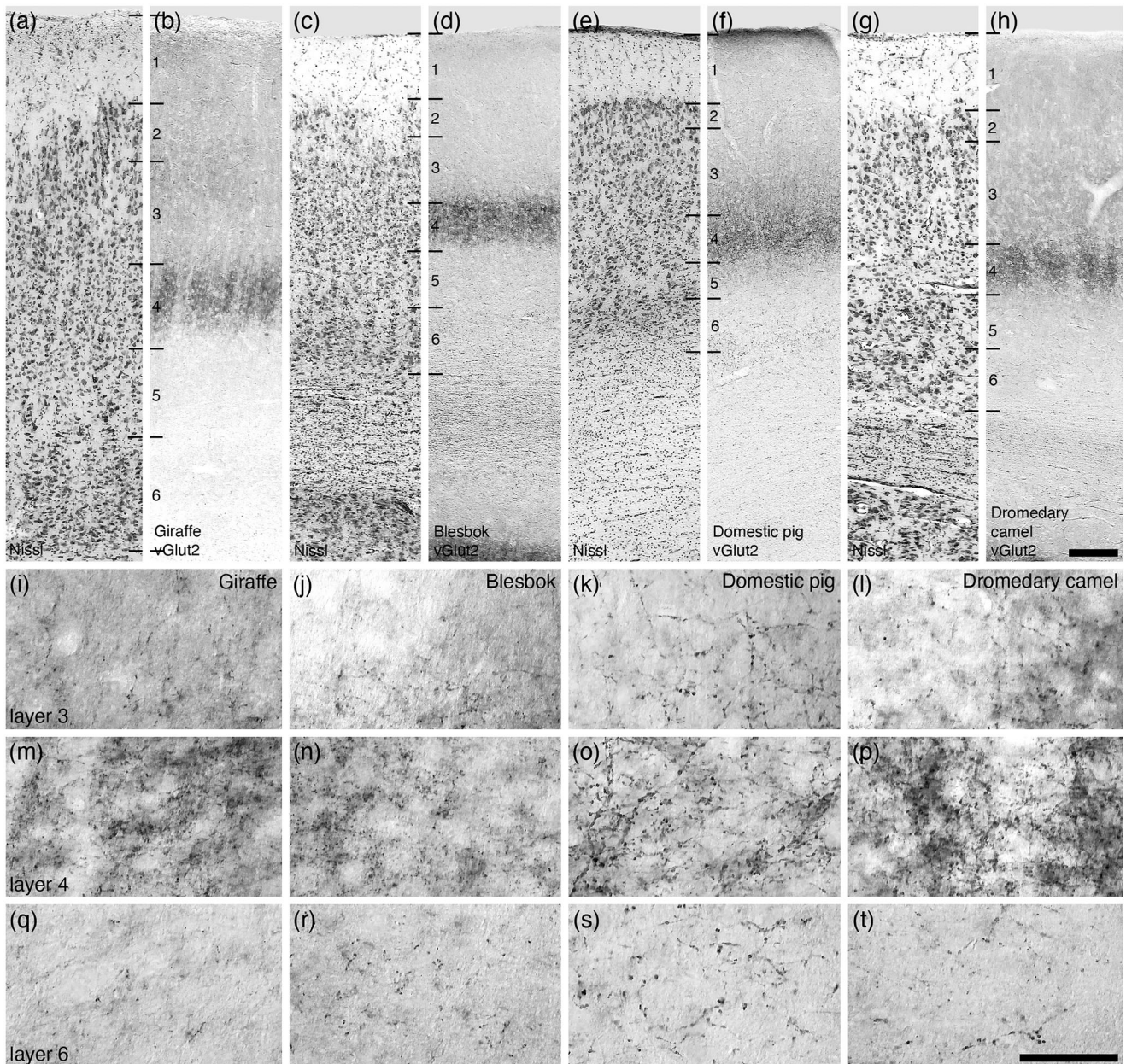


FIGURE 3 | Photomicrographs of Nissl (a, c, e, g) and vGlut2 (b, d, f, h, i–t) stained sections through the occipital cortex of the giraffe (a, b, i, m, q), blesbok (c, d, j, n, r), domestic pig (e, f, k, o, s), and dromedary camel (g, h, l, p, t). In all images, the pial surface is to the top of the image. Layer demarcations are indicated by thin horizontal black lines. Although vGlut2-immunopositive axonal terminals were observed in all layers, the most significant terminal densities were observed in layers 3, 4, and 6. Note that the ascending vGlut2-immunopositive terminal arbors do not extend in a substantive way into layer 2. Scale bar in (h) = 200 μ m and applies to (a)–(h). Scale bar in (t) = 50 μ m and applies to (i)–(t). vGlut2, vesicular glutamate transporter 2.

3.3.2 | vGlut2 Axonal Terminal Laminar Densities in Cortices With an Atypical Layer 4—African Elephant, Cetacean, and River Hippopotamus Cortex

vGlut2-immunopositive axonal terminals were observed in all layers of the occipital and temporal cerebral cortex examined in the African elephant (Figure 8), minke whale (Figure 9), harbor porpoise (Figure 10), and river hippopotamus (Figure 11), although the relative overall densities of these terminals were higher in the African elephant (Figure 8) compared to the cetaceans and hippopotamus (Figures 9–11). Despite this

increased relative density in the African elephant, the laminar pattern of vGlut2-immunopositive axonal terminals was similar across these four species, where an *atypical* layer 4 is observed throughout the cerebral cortex. In all four species, layer 3 could be readily subdivided into an outer (3o) and inner (3i) sub-lamina. For the African elephant, 3o was distinguished from 3i by having a lower density of neurons, an absence of PV-, CB-, and CR-immunopositive neurons that are present in 3i, and a slightly higher density of NFH-immunopositive neural structures (Figure 8c–i). In the minke whale, 3o exhibited a lower density of neurons than 3i, with PV-, CB-, and CR-immunopositive neurons

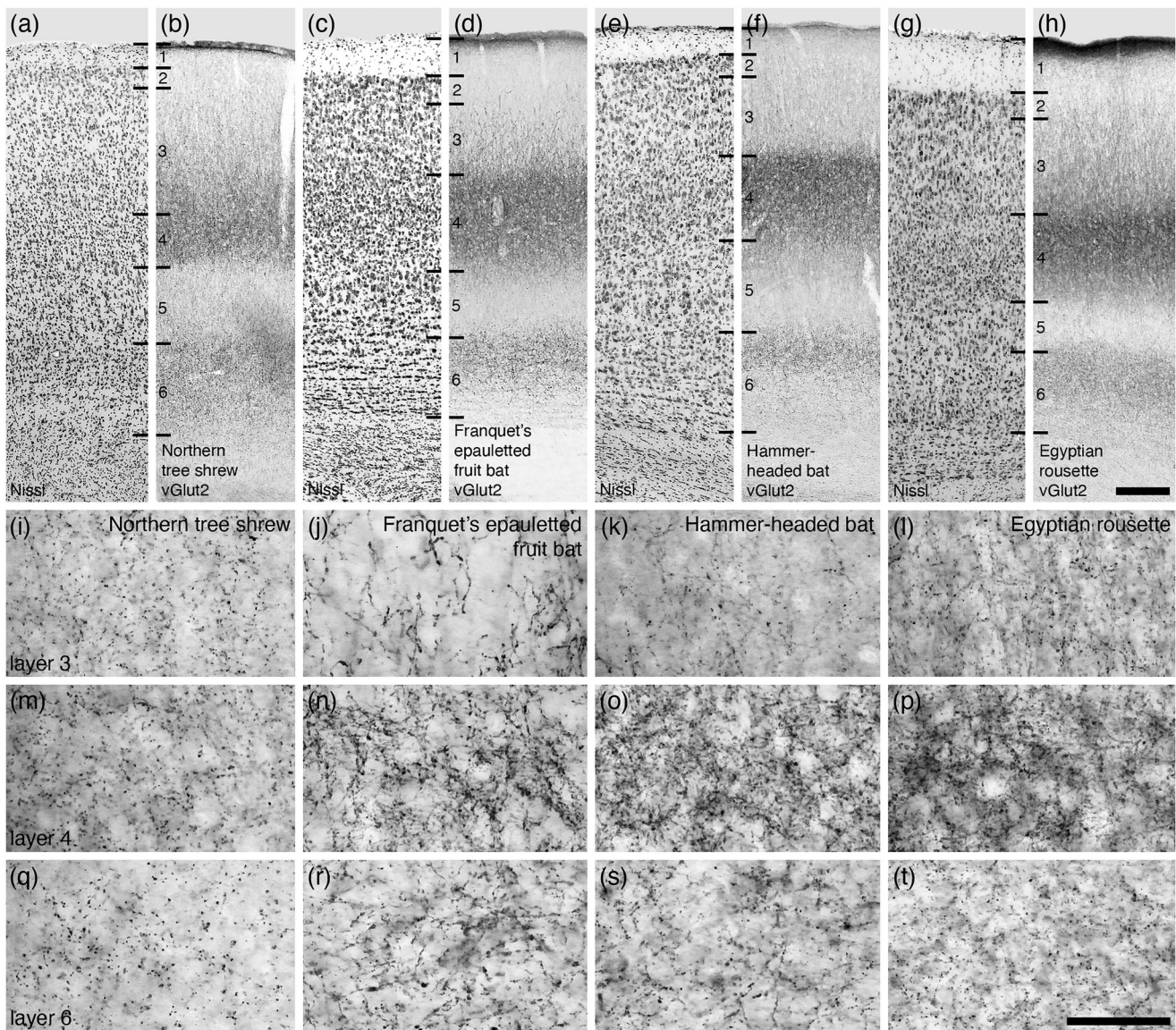


FIGURE 4 | Photomicrographs of Nissl (a, c, e, g) and vGlut2 (b, d, f, h, i–t) stained sections through the occipital cortex of the northern tree shrew (a, b, i, m, q), Franquet's epauletted fruit bat (c, d, j, n, r), hammer-headed bat (e, f, k, o, s) and Egyptian rousette (g, h, l, p, t). In all images, the pial surface is to the top of the image. Layer demarcations are indicated by thin horizontal black lines. Although vGlut2-immunopositive axonal terminals were observed in all layers, the most significant terminal densities were observed in layers 3, 4, and 6. Note that the ascending vGlut2-immunopositive terminal arbors do not extend in a substantive way into layer 2. Scale bar in (h) = 200 μ m and applies to (a)–(b). Scale bar in (t) = 50 μ m and applies to (i)–(t). vGlut2, vesicular glutamate transporter 2.

being observed in higher density in 3o than 3i (Figure 9a–f). In the harbor porpoise, no obvious differences in neuronal densities were observed between 3o and 3i, but PV-immunopositive neurons were absent from 3o, whereas they formed a clear population of 3i (Figure 10a–c). In the river hippopotamus, the distinction between 3o and 3i was not as clear as in these other species, but it was noted that 3o exhibited a higher relative neuronal density than 3i, and although both sublamina contained PV-immunopositive neurons, the relative density was lower in 3o than 3i (Figure 11a–c). In all four species, the greatest relative density of vGlut2-immunopositive axonal terminals was noted in 3i, whereas a slightly lower density was noted in 3o (Figures 9–11). The density of vGlut2-immunopositive axonal terminals was low in all other cortical layers (Figures 9–11).

4 | Discussion

In the current study, we examined the laminar distribution of vGlut2-immunopositive axonal terminals in selected regions of the neocortex of 31 eutherian mammals spanning a broad phylogenetic distribution (Table 1). These vGlut2-immunopositive axonal terminals are reported to represent the ascending core, or first order, thalamocortical projections to the neocortex (Balaram and Kaas 2014; Bryant et al. 2012; Graziano et al. 2008; Hackett and de la Mothe 2009; Jones 1998, 2007; Kaneko et al. 2002; Marion et al. 2013; Nahmani and Erisir 2005; Travis 2012; Wong and Kaas 2008, 2009). The core thalamocortical projection is often depicted as terminating in layers 4 and inner layer 3 of the mammalian neocortex, but certain neocortical areas, such as the primary motor cortex, and certain species, such as elephants,

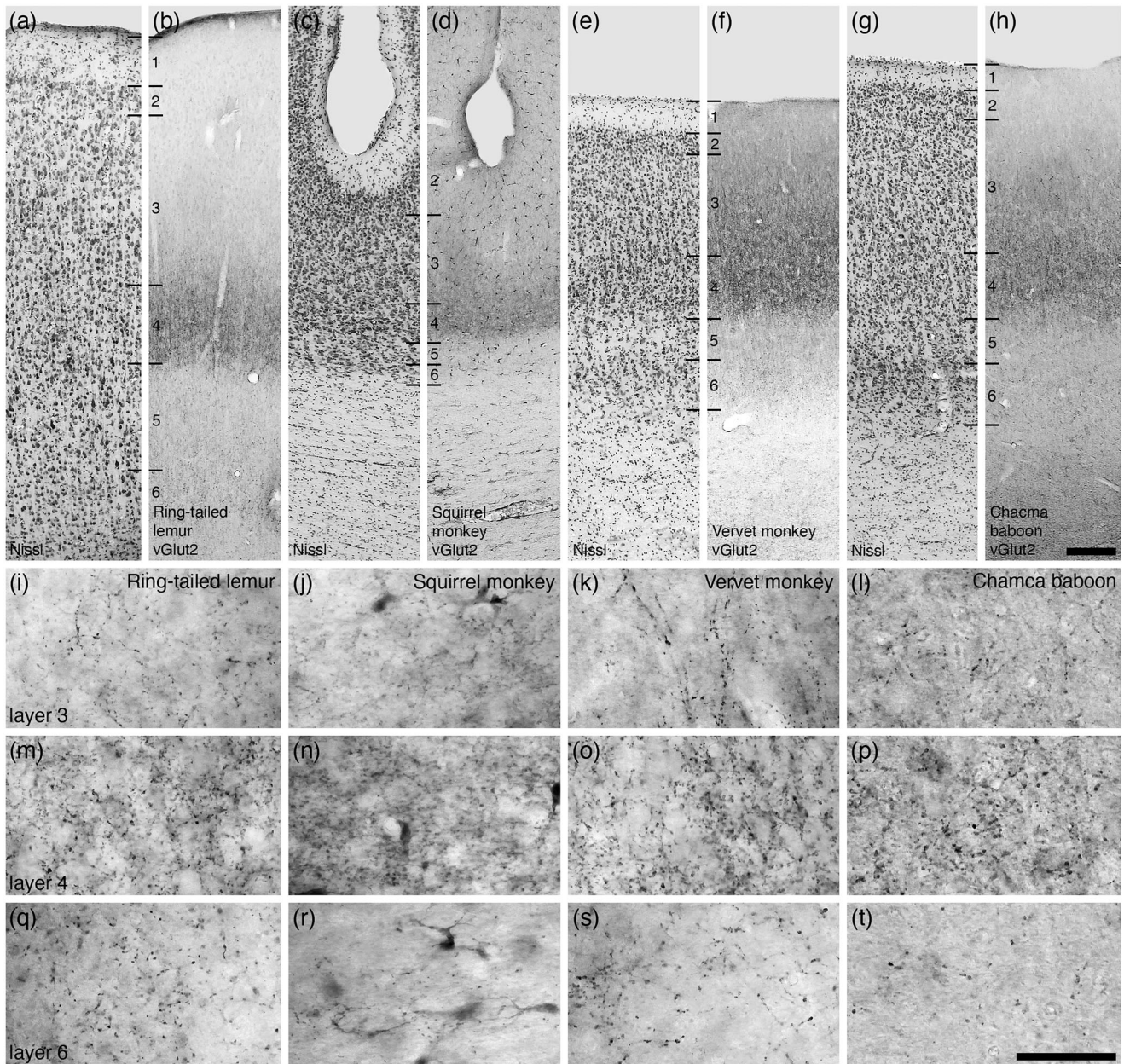


FIGURE 5 | Photomicrographs of Nissl (a, c, e, g) and vGlut2 (b, d, f, h, i–t) stained sections through the primary somatosensory cortex (area 3b) of the ring-tailed lemur (a, b, i, m, q), squirrel monkey (c, d, j, n, r), vervet monkey (e, f, k, o, s), and chacma baboon (g, h, l, p, t). In all images, the pial surface is to the top of the image. Layer demarcations are indicated by thin horizontal black lines. Although vGlut2-immunopositive axonal terminals were observed in all layers, the most significant terminal densities were observed in layers 3, 4, and 6. Scale bar in (h) = 200 μ m and applies to (a)–(h). Scale bar in (t) = 50 μ m and applies to (i)–(t). vGlut2, vesicular glutamate transporter 2.

cetaceans, and hippopotami, lack a cytoarchitecturally distinct layer 4. Here we examined where the core thalamocortical projections terminate in such neocortical areas and species, while contextualizing our findings against neocortical areas in species where there is a cytoarchitecturally distinct layer 4, or where layer 4 exhibits sublamination such as in the primate primary visual cortex. Our observations indicated that the core thalamocortical projections, as revealed with vGlut2 immunohistochemistry, do vary significantly across species, at times reflecting phylogenetic relationships, both with and without a cytoarchitecturally distinct layer 4 (Figure 12). These variations in the core thalamocortical projections and the appearance of layer 4 likely have significant

perceptual and behavioral effects in the species in which these are found.

Neocortical layer 4 has been reported to be absent, or cytoarchitecturally indistinct, in the mammalian primary motor cortex, and throughout the entire neocortex in species such as elephants, cetaceans, and hippopotami (Butti et al. 2014; Furutani 2008; Glezer et al. 1988; Hakeem et al. 2009; Jacobs et al. 2011; Major 1879; Manger 2006). Despite these reports, it should be noted that various studies have indicated that in primary motor cortex, layer 4: (1) is prominent during development but becomes increasingly less prominent in the first postnatal months (Amunts, Schleicher,

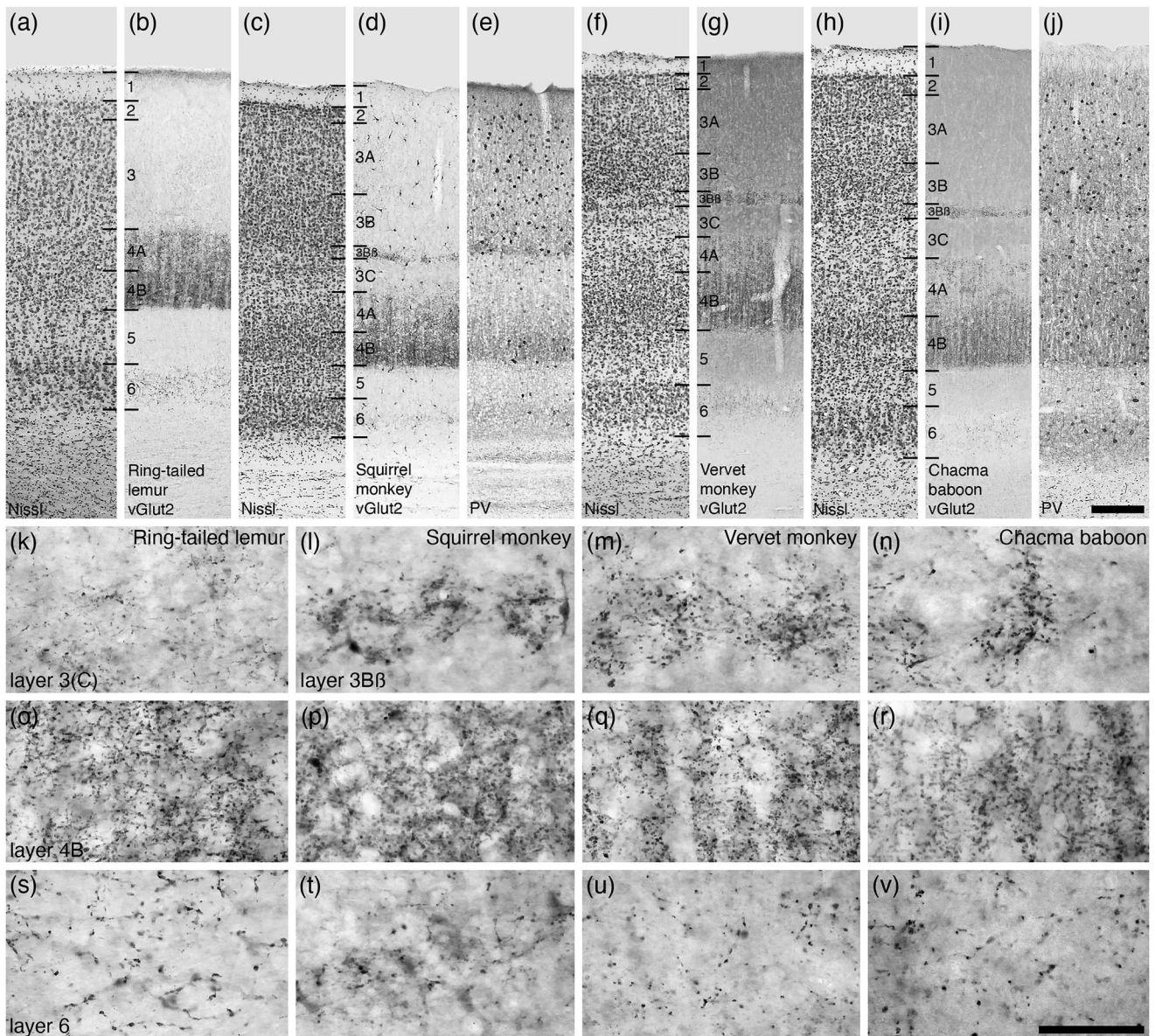


FIGURE 6 | Photomicrographs of Nissl (a, c, f, h), vGlut2 (b, d, g, i, k–v), and PV (e, j) stained sections through the primary visual cortex of the ring-tailed lemur (a, b, k, o, s), squirrel monkey (c, d, e, l, p, t), vervet monkey (f, g, m, q, u), and chacma baboon (h, i, j, n, r, v). In all images, the pial surface is to the top of the image. Layer demarcations follow that outlined by Balamam and Kaas (2014). Although vGlut2-immunopositive axonal terminals were observed in all layers, the most significant terminal densities were observed in deep layer 3 (presumably layer 3C) of the ring-tailed lemur (k), and layer 3Bβ of the other primate species (l–n), layer 4B in all four species (q–r), and layer 6 (s–v). Scale bar in (j) = 200 μm and applies to (a)–(j). Scale bar in (v) = 50 μm and applies to (k)–(v). PV, parvalbumin; vGlut2, vesicular glutamate transporter 2.

and Zilles, 1997; Brodman 1909; Conel 1951; Marin-Padilla 1970); (2) is present in the primary motor cortex of the laboratory rat (Skoglund, Pascher, and Berthold 1997) and adult primates (García-Cabezas, and Barbas 2014); and (3) is represented functionally through analogous, or perhaps homologous, intracortical circuitry (Yamawaki et al. 2014). It should also be noted that it has been reported that layer 4 is present in the developing visual cortex of dolphins (Garey and Leuba 1986), and that our NFH immunostaining in the African elephant cerebral cortex (Figure 8i) could be interpreted as reflecting the presence of a layer 4 following the reasoning presented by García-Cabezas and Barbas (2014). Despite these differing reports, all agree that in the primary motor cortex and in certain species, there is no

cytoarchitecturally distinct layer 4. To avoid potential confusion, here we refer to layer 4 as being cytoarchitecturally indistinct, or perhaps absent, rather than being definitive about the presence or absence of this neocortical layer. Further research is required to be definitive about the presence or absence of layer 4 in certain neocortical regions and the entire neocortex of certain species.

4.1 | Study Limitations

Although our study examines several eutherian mammal species and cortical areas, it is by no means a comprehensive study. Examining the thalamocortical laminar termination patterns

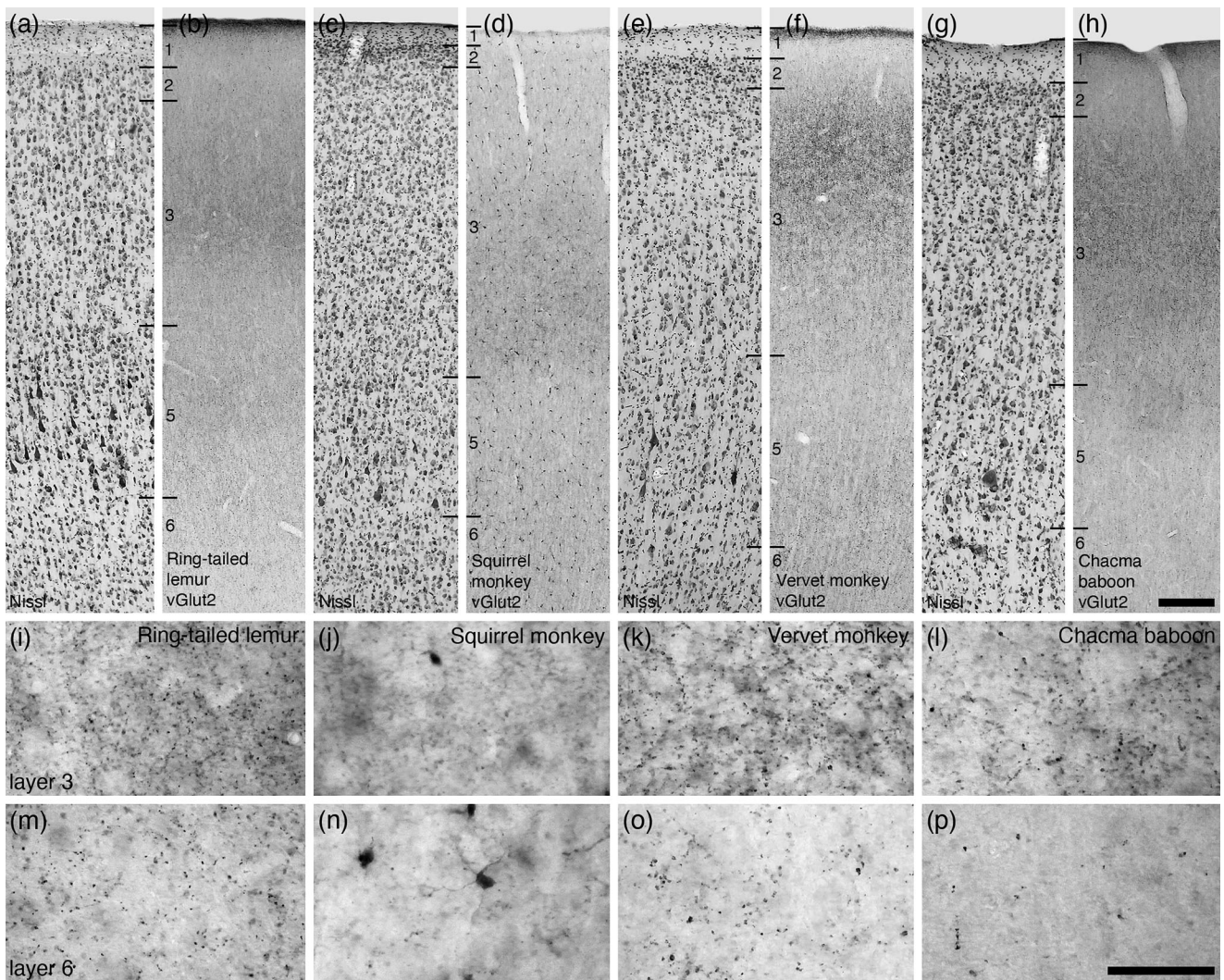


FIGURE 7 | Photomicrographs of Nissl (a, c, e, g) and vGlut2 (b, d, f, h, i–p) stained sections through the primary motor cortex (area M1) of the ring-tailed lemur (a, b, i, m), squirrel monkey (c, d, j, n), vervet monkey (e, f, k, o), and chacma baboon (g, h, l, p). In all images, the pial surface is to the top of the image. Layer demarcations are indicated by thin horizontal black lines. Note the absence of a cytoarchitecturally distinct layer 4. Although vGlut2-immunopositive axonal terminals were observed in all layers, the most significant terminal densities were observed in layers 3 and 6. Scale bar in (h) = 200 μ m and applies to (a)–(h). Scale bar in (p) = 50 μ m and applies to (i)–(p). vGlut2, vesicular glutamate transporter 2.

across a broader range of species and cortical areas may reveal more patterns than those reported herein. This means that the current study cannot be considered exhaustive, but rather indicative, of the potential variations that may be present in the core thalamocortical projection in mammal neocortical areas; however, the range of neocortical areas and species studied, including those with *specialized* and *atypical* layer 4 morphology, does provide important information that alters general concepts of the thalamocortical projection system. The current study is purely qualitative in nature in that no quantification of core thalamocortical terminal densities was undertaken. Quantification of terminal densities may provide numerical data that can reveal subtle differences between species that may have been missed with our qualitative approach, but we do provide substantial iconography of the vGlut2-immunostained tissue in many of the species and cortical layers to support the qualitative statements made. In this sense, our qualitative observations should be considered what are likely to be the most probable observations that would be made in the neocortical areas

and species examined. Future studies employing quantification would likely reveal an increased number of thalamocortical laminar projection patterns. It is also important to note that at any specific time, even though a neuron may be capable of producing a specific transporter, it may not be doing so. Thus, at the time of death of the animals used in this study, it may be the case that certain neurons that can express vGlut2 were not doing so, thus leading to a false negative observation. Although we generalize our results, we do so with caution, and temper our conclusions cognizant of these potential confounding factors.

4.2 | Broadening the Definition of the Core Thalamocortical Projection

Jones (1998) proposed, based primarily on observations of the somatosensory and auditory systems of primates, that the thalamocortical projection is subdivided into core and matrix portions

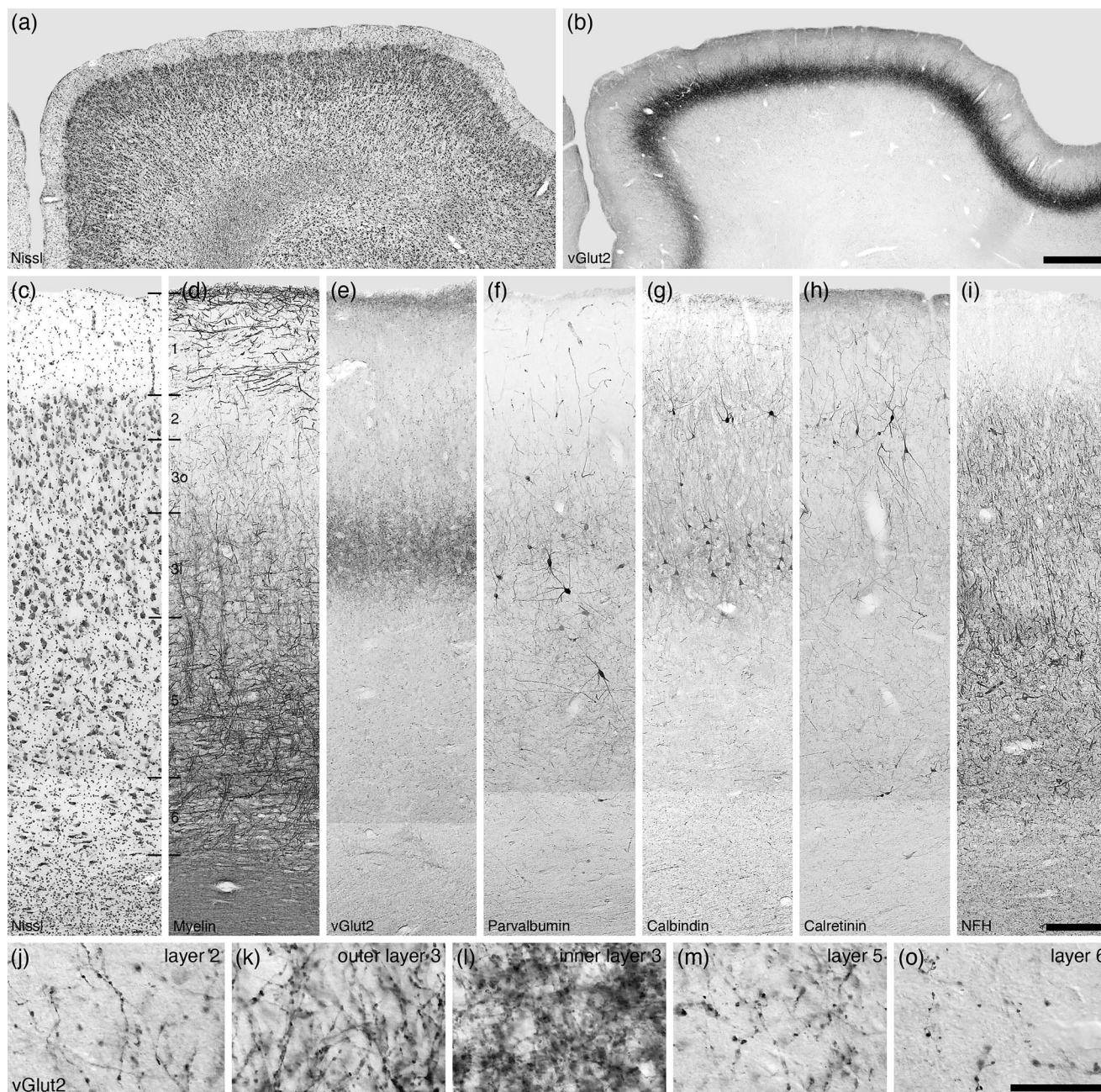


FIGURE 8 | Photomicrographs of Nissl (a), vGlut2 (b, e, j–o), myelin (d), PV (f), CB (g), CR (h), and NFH (i) stained sections through the occipital cortex of the African elephant. In all images, the pial surface is to the top of the image. Layer demarcations are indicated by thin horizontal black lines. Although vGlut2-immunopositive axonal terminals were observed in all layers (j–o), the most significant terminal densities were observed in both outer layer 3 (3o) (k) and inner layer 3 (3i) (l). Scale bar in (b) = 1 mm and applies to (a) and (b). Scale bar in (i) = 200 μ m and applies to (c)–(i). Scale bar in (o) = 50 μ m and applies to (j)–(o). NFH, neurofilament H; vGlut2, vesicular glutamate transporter 2.

(termed first and higher order projections, respectively, by Sherman and Guillery (2002)), the core representing the pathway through which ascending sensory information is passed to the middle layers (layers 4 and inner layer 3) of the neocortex. To reveal this core thalamocortical projection across species, in the current study, we used an antibody targeting vGlut2 that has been shown to label the core thalamocortical projection (Balaram and Kaas 2014; Balaram et al. 2013, 2015; Bryant et al. 2012; Graziano et al. 2008; Hackett and de la Mothe 2009; Kaneko et al. 2002; Marion et al. 2013; Nahmani and Erisir 2005; Wong and Kaas 2008, 2009). In the species examined in the current

study, we observed six distinctly different patterns of the laminar distribution of the core thalamocortical projection system (Figure 12). Jones (1998) highlighted that this core projection might differ in non-primate species, which concurs with our findings. Although we have revealed six different patterns of the core thalamocortical projection in the species studied, it is likely that more patterns exist in unstudied species. Thus, as indicated by Jones (1998), we cannot say that any specific pattern of core thalamocortical projection is “mammalian,” but rather that many patterns are likely to occur. This does not undermine the concept of core and matrix thalamocortical projections that

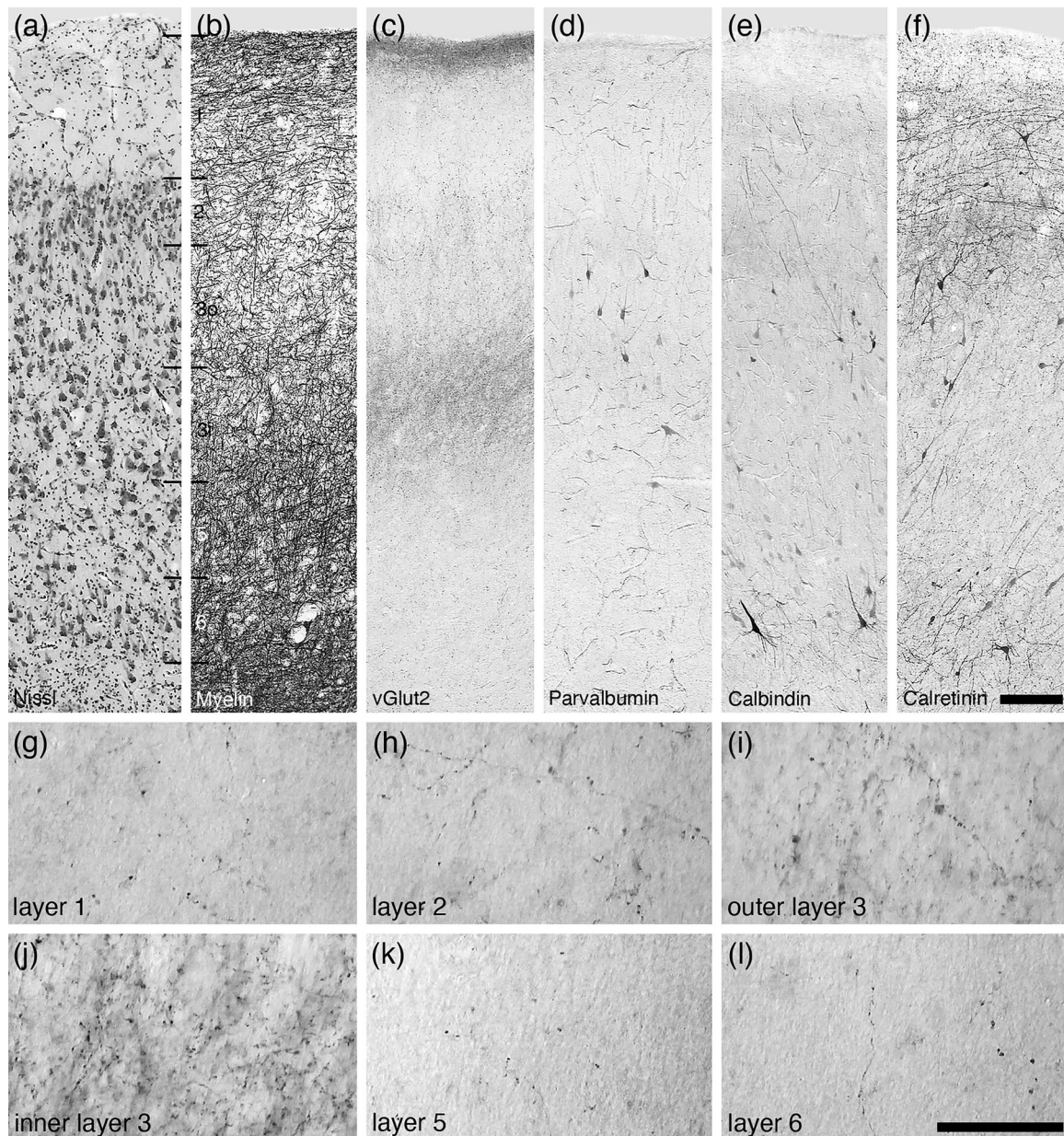


FIGURE 9 | Photomicrographs of Nissl (a), myelin (b), vGlut2 (c, g–l), PV (d), CB (e), and CR (f) stained sections through the occipital cortex of the minke whale. In all images, the pial surface is to the top of the image. Layer demarcations are indicated by thin horizontal black lines. Although vGlut2-immunopositive axonal terminals were observed in all layers (g–l), the most significant terminal densities were observed in both outer layer 3 (3o) (k) and especially so in inner layer 3 (3i) (l). Scale bar in (f) = 200 μ m and applies to (a)–(f). Scale bar in (l) = 50 μ m and applies to (g)–(l). vGlut2, vesicular glutamate transporter 2.

appear to be a consistent feature across mammals, but the precise manner in which the core thalamocortical projections terminate in the neocortex can and does vary, and we must be cognizant of this variation when examining different mammal brains. Despite this, the core and matrix thalamocortical projections as outlined by Jones (1998) are likely to be the patterns most commonly observed across mammals. Furthermore, it is likely that the neural information that forms the basis of perception is transmitted by the core thalamocortical projection, which, when tied to variations across species, indicates that the perceptual worlds of species that exhibit a core thalamocortical projection different from that seen in primates, may be quite different from our own.

4.3 | Functional Correlates of Core Thalamocortical Projections and Layer 4 Variations

The most commonly observed pattern of core thalamocortical projections was coincident with a *typical* layer 4 that is not sublaminate and comprised small granular neurons. Although the core thalamocortical projections in this pattern terminate primarily on the small granular cells of layer 4, they also terminate on the larger pyramidal neurons forming the inner portion of layer 3. It is important to note that a single core thalamocortical axon arborizes extensively within the cerebral cortex, with the terminals of this single axon diverging horizontally over a distance greater than 500 μ m, sometimes up to

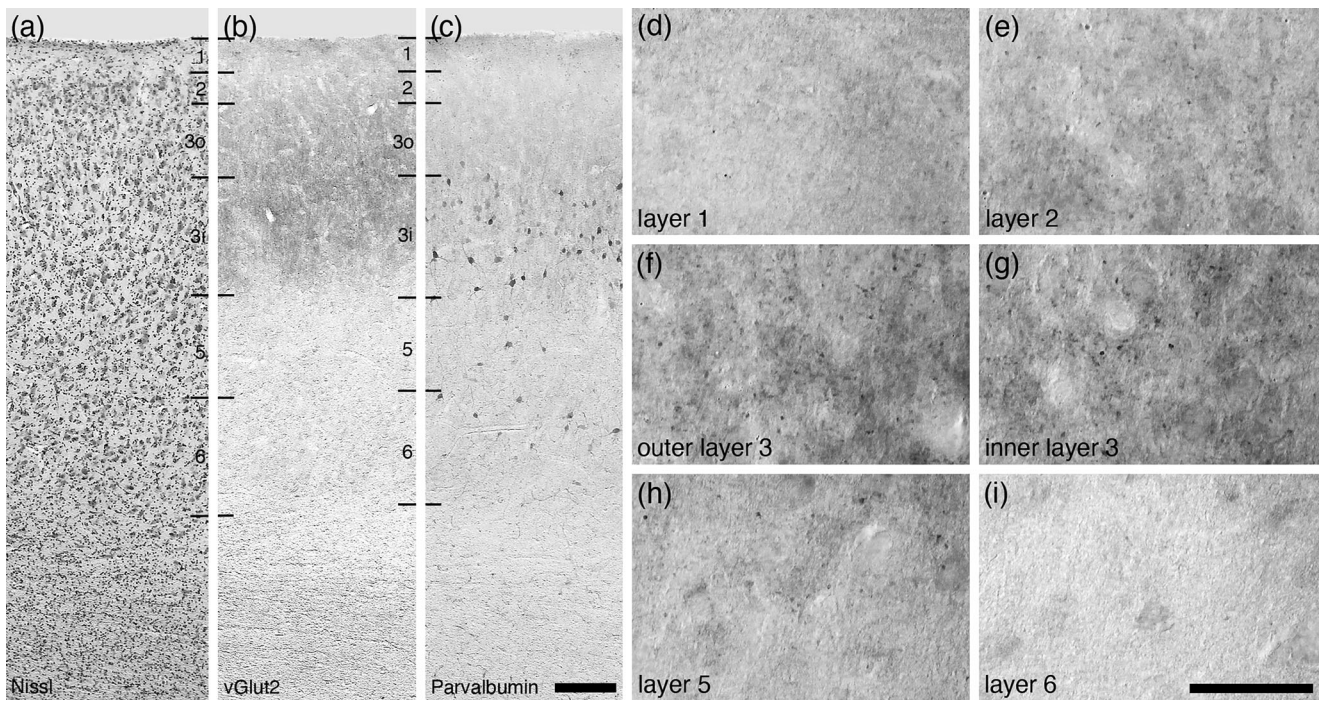


FIGURE 10 | Photomicrographs of Nissl (a), vGlut2 (b, d–i), and PV (c) stained sections through the temporal cortex of the harbour porpoise. In all images, the pial surface is to the top of the image. Layer demarcations are indicated by thin horizontal black lines. Although vGlut2-immunopositive axonal terminals were observed in all layers, the most substantial terminal densities were observed in both outer layer 3 (3o) (f) and inner layer 3 (3i) (g). Scale bar in (c) = 200 μ m and applies to (a)–(c). Scale bar in (i) = 50 μ m and applies to (d)–(i). vGlut2, vesicular glutamate transporter 2.

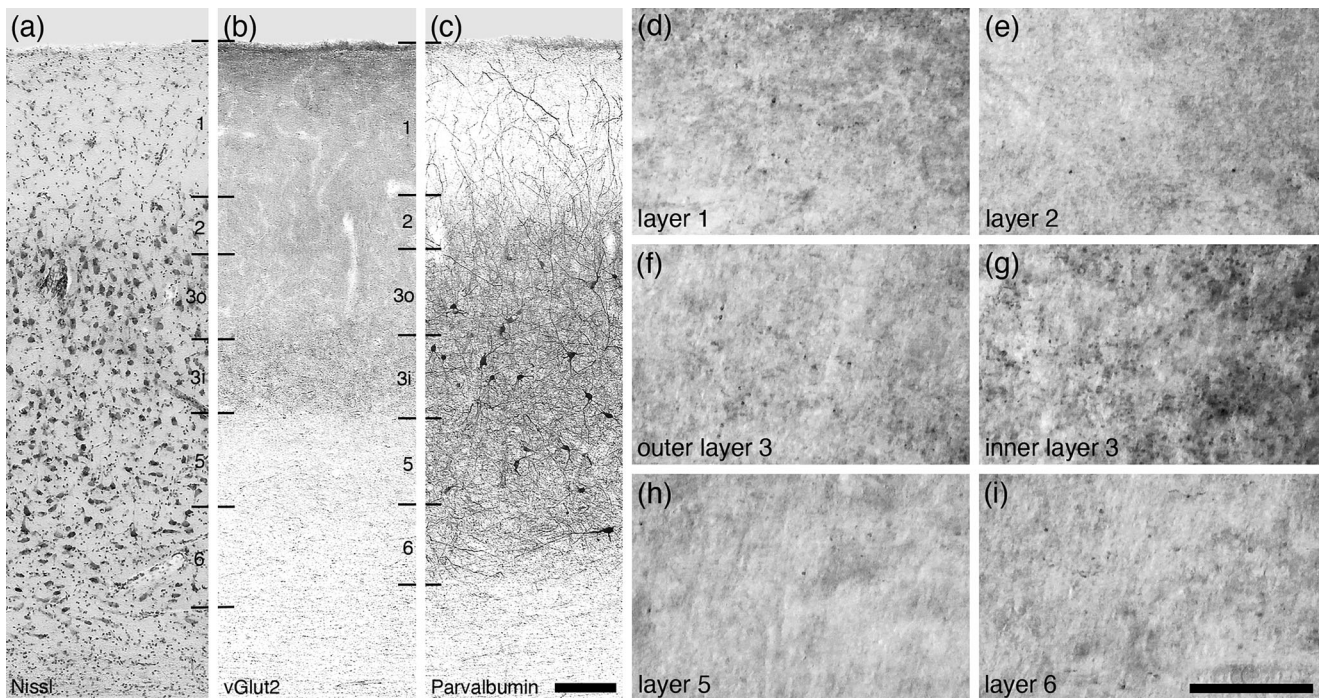


FIGURE 11 | Photomicrographs of Nissl (a), vGlut2 (b, d–i), and PV (c) stained sections through the occipital cortex of the river hippopotamus. In all images, the pial surface is to the top of the image. Layer demarcations are indicated by thin horizontal black lines. Although vGlut2-immunopositive axonal terminals were observed in all layers, moderate terminal densities were observed in outer layer 3 (3o) (f) and the most substantial terminal densities were observed in inner layer 3 (3i) (g). Scale bar in (c) = 200 μ m and applies to (a)–(c). Scale bar in (i) = 50 μ m and applies to (d)–(i). vGlut2, vesicular glutamate transporter 2.

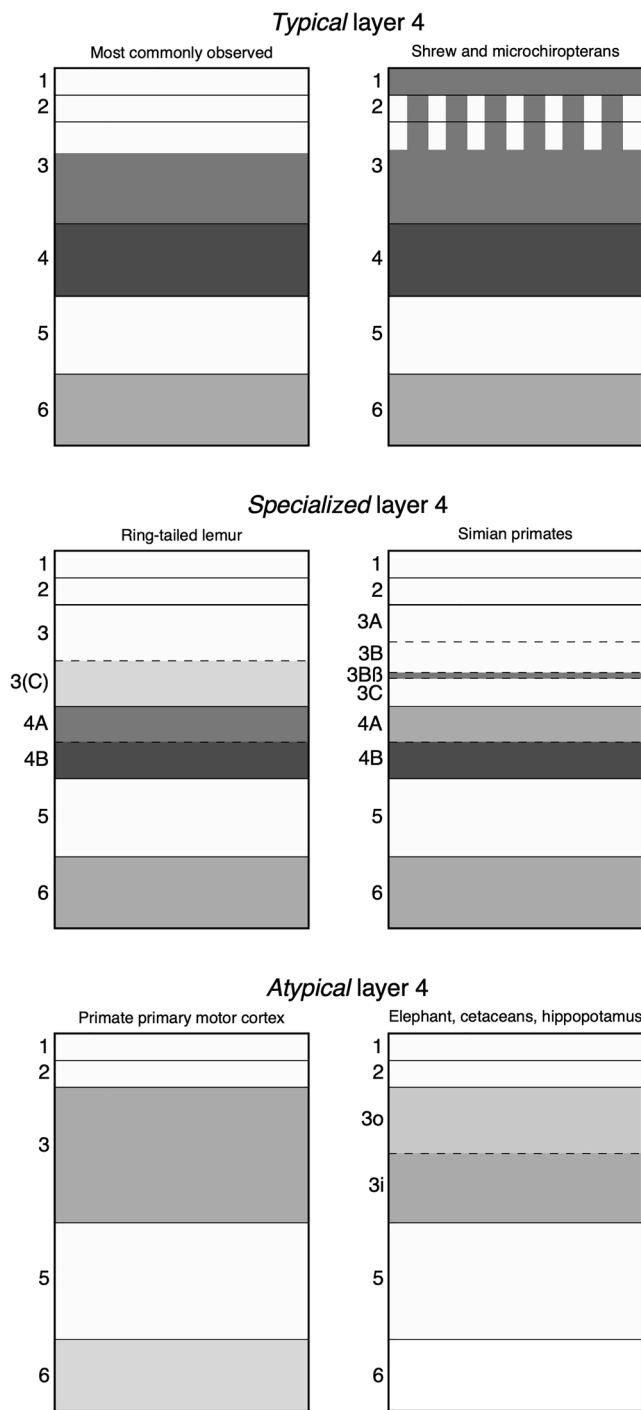


FIGURE 12 | Diagrammatic summary of the findings detailed in the current study. Six different patterns of core thalamic inputs to the cerebral cortex were observed across the species studies. Associated with cortices exhibiting a *typical* layer 4 (see text for definition) was that most commonly observed and that specifically observed in the greater forest shrew and microchiropterans (upper row). Within primate primary visual cortex, area V1, where a *specialized* layer 4 was observed (see text for definition), two patterns of thalamocortical terminations were observed, that associated with prosimian and simian primates (middle row). In cortical areas and species without a cytoarchitecturally distinct layer 4, that we term an *atypical* layer 4 (see text for definition), again two distinct laminar patterns of vGlut2-immunopositive axonal terminals were observed, that associated with the primary motor cortex in primates, and that found throughout the cortex of African elephants, cetaceans, and

the river hippopotamus (lower row). The diagrams presented here are not to scale, and the shades represent relative densities (darker shading indicating greater density) based on qualitative assessment.

several millimeters, as well as across several cortical layers (e.g., Aumann, Ivanusic, and Horne 1998; Kaneko 2013; Kuramoto et al. 2009; Ohno et al. 2012; Rodriguez-Moreno et al. 2020). This means that each thalamocortical axon can communicate information spanning a greater horizontal distance across the cerebral cortex than even the largest pyramidal neuron dendritic field areas/volumes observed in mammals (e.g., Elston and Manger 2014; Elston et al. 2006; Jacobs et al. 2011, 2017). The dendritic field extent of layer 4 granular neurons is typically smaller than those of layer 3 pyramidal neurons (e.g., Jacobs et al. 2015; Meyer, González-Hernández, and Ferres-Torres 1989). This interlaminar variation in dendritic field extent is reflected in the size of neuronal receptive fields recorded in different cortical layers, where the receptive fields in layer 4 are smaller than those recorded in other layers (e.g., Foffani, Chapin, and Moxon 2008; Killackey and Ebner 1972; Sur, Garraghty, and Bruce 1985). These observations indicate that the same core thalamocortical input may be involved in different, but distinct, neocortical processes. Layer 4 is likely to be involved in the process of decorrelation of incoming thalamocortical neural information, allowing specific aspects of the correlated, or overlapping, thalamocortical input to be segregated into component parts with fine-tuning curves, that is, small receptive fields (e.g., Barron and Mourmourakis 2024). This would then allow for very specific aspects of incoming neural information to be passed to the supragranular layers for further processing. The core thalamocortical input to layer 3, while lacking specificity in terms of the tuning curve of neuronal responses, that is, large receptive fields, is likely to be involved in coding complex temporal aspects of incoming neural information (e.g., Foffani et al. 2008). Thus, in the species with a *typical* layer 4 and the most commonly observed pattern of core thalamocortical input, processing in the cerebral cortex provides a combination of specificity (layer 4) and temporality (layer 3), both of which are important in terms of perception and the production of behavior. But what happens when there are variations either in the pattern of core thalamocortical input or cytoarchitecture of layer 4?

In the greater forest shrew and the microchiropterans studied, a *typical* layer 4 was present, but the core thalamocortical projection labeled by vGlut2 immunohistochemistry exhibited both the most commonly observed pattern and a significant projection to the upper cortical layers, especially layer 1. Neocortical layer 1 is known to play a significant role in both top-down and bottom-up integration of neocortical processing networks contributing to perception, integration, attention, and learning (e.g., Schuman et al. 2021). The addition of significant core thalamocortical inputs to this layer may augment the capacity of layer 1 to influence perception and motor timing control in the millisecond to second range (e.g., Moss and Sinha 2003), perhaps allowing these species to respond more rapidly and with greater precision to the evasive actions of prey.

In the primary visual cortex of the four species of primates, in agreement with earlier reports (e.g., Balaram and Kaas 2014; Balaram et al. 2013), a *specialized* layer 4 that exhibited

sublamination (into a superficial sublayer 4A and a deep sublayer 4B) was observed. Layer 3 of this primate neocortical area was also sublaminated, in the prosimian ring-tailed lemur into two distinct sublayers and in the simian primates into four sublayers. The pattern of core thalamocortical projections in primate primary visual cortex exhibited clear differences to the pattern most commonly observed. In all primates, sublayer 4B exhibited the greatest density of core thalamocortical projections, followed by sublayer 4A. In the ring-tailed lemur, sublamina 3(C) was in receipt of core thalamocortical projections, while in the simians studied, sublamina 3B β exhibited a very specific high-density core thalamocortical projection. In the primary visual cortex of primates, sublayer 4B is known to be in receipt of the P pathway which is associated with high acuity achromatic vision and red/green color vision (Lee, Martin, and Grünert 2010; Nassi and Callaway 2009), whereas sublayer 4A is in receipt of the M pathway that is involved in motion detection (Croner and Kaplan 1995; Kaplan and Shapely 1986). The segregation of these two aspects of visual information, among other specializations of primate primary visual cortex, likely augments the capacity of this cortical area to decorrelate these potentially overlapping core thalamocortical inputs (Barron and Mourmourakis 2024). This may then lead to more precise information regarding motion, color, and acuity, being available to the visual perceptual network of the primate brain. Such neural changes may help the frugivorous primates to select fruits using subtle color cues (e.g., Barton 1998) and move more rapidly and accurately through their environment.

Two different patterns of core thalamocortical projections were associated with an *atypical* layer 4, where if a layer 4 is present it is not cytoarchitecturally distinct. In the primary motor cortex of the primates studied, core thalamocortical projections were found evenly distributed throughout layer 3. This indicates that the direct core thalamocortical projections are unlikely to undergo decorrelation as observed in cortical areas where a layer 4 is present. Yet, movements made by primates, and indeed many other mammals, can be incredibly precise. There are two important aspects regarding primary motor cortex in this context: (1) Primary motor cortex is the terminal cortical area of the motor system that executes voluntary motor actions, rather than being involved in the planning of actions, with the specificity in the planning of motor outputs being achieved in other regions of the brain, including the premotor cortical areas, striatopallidal complex, and cerebellum (e.g., Geyer, Matelli, Luppino, and Zilles 2000; Swanson 2011); and (2) the decorrelation of sensory inputs required for the planning of motor actions, especially those based on conscious perception, is likely to have occurred elsewhere in the cerebral cortex where a cytoarchitecturally distinct layer 4 is present. In this sense, there does not appear to be a need for the decorrelative properties of layer 4 in the primary motor cortex, and this may be the reason that no cytoarchitecturally distinct layer 4 is found in the primary motor cortex of mammals. The core thalamocortical projections to layer 3 of the primate primary motor cortex may be involved in the important temporal aspects, including feedback, of voluntary movements.

In the second example of an *atypical* layer 4, observed in the African elephant, minke whale, harbor porpoise, and river hippopotamus, the core thalamocortical projections were most dense in inner layer 3 (3i) and slightly less dense in outer layer 3

(3o). The remaining layers (1, 2, 5, 6) exhibited very low densities of core thalamocortical projections. This pattern is different from that seen in primate primary motor cortex, as the *atypical* layer 4 and pattern of core thalamocortical inputs is found across the entire neocortex, including primary sensory areas (Butti et al. 2014; Furutani 2008; Glezer et al. 1988; Hakeem et al. 2009; Jacobs et al. 2011; Major 1879; Manger 2006). Thus, if layer 4 is truly absent in these species, the decorrelation, or specification, of sensory inputs achieved by layer 4 that is passed to the conscious perceptual landscape generated by the brains of these mammals is absent. This does not mean that elephants, cetaceans, and hippopotami do not respond behaviorally to very specific sensory stimuli, as sensory stimuli may be decorrelated in non-cortical regions of the brain, such as the inferior colliculi (e.g., Glezer, Hof, and Morgane 1998), before being passed on to the neocortex. The presence of the core thalamocortical projections to layer 3 in these species indicates that the temporal aspects of cortical processing are still present. It has been proposed that adding layers to neural processing networks will add cognitive capacity to these networks (e.g., Barron and Mourmourakis 2024), with the inverse presumably detracting from cognitive capacities; however, if decorrelations were to occur in other brain regions prior to neocortical processing, the inverse argument is not supported. What is interesting in these cases of an *atypical* layer 4 is whether very specific, or decorrelated, sensory input is available to the cortical networks that generate conscious perceptions. At present, a meaningful answer cannot be provided, with both correlated and non-correlated sensory inputs potentially being available to the neocortex of these species. Understanding this dichotomy will be important to developing an understanding of the conscious perceptual world of mammals with an *atypical* layer 4.

4.4 | Phylogenetic Aspects and the Evolution of Variations in the Appearance of Layer 4 and the Core Thalamocortical Projection Patterns

The variations noted in both layer 4 and the core thalamocortical projections were often associated with specific phylogenetic lineages. Although both the most commonly observed patterns of core thalamocortical projections, and that observed in primate primary motor cortex, are likely to be found in most mammalian cortices and the primary motor cortex of most mammalian species, respectively, the variations do appear to correlate with specific phylogenetic affinities. The unusual pattern of core thalamocortical projections in the greater forest shrew and microchiropterans suggests a potential phylogenetic affinity for these two mammalian groups, supporting earlier suggestions based on studies of the brains of the Soricidae and microchiropterans (Dell et al. 2010). However, it must be noted that a similar thalamocortical projection, revealed by vGlut2 immunohistochemistry, was observed in the monocular zone of the primary visual cortex of the tree shrew (Balaram et al. 2015), indicating that such a core thalamocortical projection may be found across a broader range of species and argues against the potential phylogenetic affinity of shrews and microchiropterans suggested. The core thalamocortical projections observed in the megachiropterans studied were quite different from that seen in the microchiropterans, adding another feature of the brain that can be argued to be supportive of the diphyletic origin of the chiroptera proposition (Dell et al. 2010; Pettigrew 1986; Pettigrew

et al. 1989). The megachiropterans revealed the most commonly observed core thalamocortical projection pattern, which was similar to that seen in the northern tree shrews studied both of which were not substantially different from the pattern of core thalamocortical projections seen in prosimian primates, including the ring-tailed lemur studied herein and the galago and mouse lemur studied by Balaram and Kaas (2014). Despite this, it is important to note that our findings in the tree shrew are quite different from that reported by Balaram and Kaas (2014) and Balaram et al. (2015), who, using vGlut2 immunostaining and other stains, show that in primary visual cortex of the tree shrew, there is a sublaminate layer 4, and a distinct layer 3B that are vGlut2 immunopositive. Indeed, our staining in the tree shrew looks very similar to the vGlut2 immunostaining of V2 in the tree shrew demonstrated by Balaram and Kaas (2014). Thus, it appears that our occipital blocks in the tree shrew (e.g., Lyon, Jain, and Kaas 1998), and perhaps in the megachiropterans (Rosa 1999), sampled extrastriate visual areas, rather than the targeted primary visual cortex. Given the proposed phylogenetic affinity of the megachiropterans to primates (Dell et al. 2010; Pettigrew 1986; Pettigrew et al. 1989), it would be interesting to examine vGlut2 immunostaining unambiguously in the primary visual cortex of megachiropterans to determine whether they show similarities or differences to the tree shrews (Balaram et al. 2015). Despite these two possible phylogenetic affinities for the diphyletic proposition of chiropteran evolution (microchiropterans aligned to the Soricidae and megachiropterans to the dermopterans) derived from studies of the brain, aspects of molecular and morphological studies propose a monophyletic origin for the chiropterans; however, the proposed phylogenetic alignment of chiropterans to other mammalian lineages diverge dramatically and variously indicate alignments with Dermoptera, Primates, Scandentia, Lagomorpha, Insectivora, Carnivora, Philodota, Tubulidentata, Artiodactyla, Cetaceans, and Perissodactyla (e.g., Amador et al. 2018; Simmons 1994; Tsagkogeorga et al. 2013). The phylogenetic affinity of the chiropterans within the mammals remains an open question.

The *specialized* sublaminate layer 4 observed in the primary visual cortex of the primates studied, along with the specialized layer 3B β observed in simian primates, coincide with an altered pattern of core thalamocortical projections. These observations were limited to the primary visual cortex of the primates and not observed in the occipital cortex of any of the other species studied, making this lineage specific as noted previously (Balaram and Kaas 2014; Balaram et al. 2013). The *atypical* layer 4, associated with an altered pattern of core thalamocortical projections in the minke whale, harbor porpoise, and river hippopotamus, reflects the phylogenetic proximity of the cetaceans and hippopotamids within the artiodactyls (Price, Bininda-Emonds, and Gittleman 2005); however, the findings in the African elephant indicate that similar patterns of an *atypical* layer 4 and modified core thalamocortical projections can evolve independently.

It is of interest to try to understand why different laminar and thalamocortical projection patterns may emerge in different lineages or independently. In terms of the primary visual cortex of primates, the differences noted in the current study and previously (Balaram and Kaas 2014; Balaram et al. 2013) appear to be correlated with the specializations of the visual system in primates as compared to other mammals (e.g., van Essen

and Anderson 1995). In contrast, the lineage-specific changes observed in the cetaceans and hippopotamids, which also appear in the phylogenetically distant African elephant, do not appear to be the result of similar sensorimotor, perceptual, or cognitive specializations shared among these species driving convergent evolution of similar neural traits. One interesting, although admittedly tenuous, correlation is that the four species studied showing an *atypical* layer 4 have unusual skin—pachydermia in the river hippopotamus (Luck and Wright 1964; Springer et al. 2021) and African elephant (Martins et al. 2018; Smith 1890), and a thickened, thermogenetic (Hashimoto et al. 2015), and blubbery skin in the cetaceans (Springer et al. 2021). The skin and brain share an early ectodermal origin (Jameson, Boulton et al. 2023); thus, perhaps alterations in the pattern/s and timing/s of gene/s expression/s leading to the development of unusual mammalian skin might have pleiotropic effects leading to the development of an *atypical* layer 4 and subsequent variation in the core thalamocortical projection laminar pattern. It is worth noting that in another mammal with unusual skin, the tree pangolin, that layer 4 also appears to be *atypical* in that the neurons are pyramidalized and may in fact be the inner layer 3 noted herein, exhibiting a pattern of core thalamocortical projections like that noted in the cetaceans, hippopotamus, and elephant studied (Imam et al. 2022). The lamination of the neocortex in rhinoceroses and tapirs, both of which have skin that has a pachydermatous character (Cave and Allbrook 1959; Murie 1871; Plochocki et al. 2017), is not yet known and thus cannot be compared here but would be of interest to determine (n.b., it has been reported that the domestic horse has a cytoarchitecturally distinct layer 4, Graic et al. 2022).

Although this skin–brain link is tenuous, the possibility that the developmental genetic variations required for the maturation of an unusual skin type are associated with a pleiotropic *atypical* cortical lamination pattern is intriguing. It would be of importance to determine whether cortical layer 4 is truly absent, or just modified (e.g., Oishi et al. 2016), in mammals with unusual skin and an *atypical* layer 4, perhaps using specific layer 4 markers such as ROR β (e.g., Clark et al. 2020) or *Protocadherin20* (Oishi et al. 2016) and in situ hybridization techniques. Further, comparing timing and expressions of genes associated with cortical layer 4 and the developing mammalian skin (e.g., D’Arcy and Kiel 2021) may be of importance in understanding the skin–brain axis (Jameson et al. 2023) and acquired skin conditions such as ichthyosis vulgaris where a subset of individuals lack specific layers of the skin (Fleckman and Brumbaugh 2002).

Author Contributions

A.B., Z.M., and P.R.M. conceptualized the study. All authors obtained and prepared brains used in this study. A.B. and P.R.M. performed the staining and analysis. A.B. and P.R.M. wrote the initial draft of the manuscript, and all authors contributed to the editing and improvement of drafts of the manuscript. All authors had full access to all data in the study and take responsibility for the integrity of the data and the accuracy of the data analysis.

Acknowledgments

The authors have nothing to report.

Ethics Statement

The animals used in this study were treated according to the guidelines of the University of Witwatersrand (Clearance number 2013/05/02B) which correspond to those of the NIH for care and use of animals in scientific experimentation.

Conflicts of Interest

The authors declare no conflicts of interest.

Data Availability Statement

Data have not been shared due to this study being based on histological sections.

References

- Amador, L. I., M. Arévalo, F. C. Almeida, S. A. Catalano, and N. P. Giannini. 2018. "Bat Systematics in the Light of Unconstrained Analyses of a Comprehensive Molecular Supermatrix." *Journal of Mammalian Evolution* 25, 37–70. <https://doi.org/10.1007/s10914-016-9363-8>.
- Amunts, K., A. Schleicher, and K. Zilles. 1997. "Persistence of Layer IV in the Primary Motor Cortex (Area 4) of Children With Cerebral Palsy." *Journal Für Hirnforschung* 38, 247–260.
- Aumann, T. D., J. Ivanusic, and M. K. Horne. 1998. "Arborisation and Termination of Single Motor Thalamocortical Axons in the Rat." *Journal of Comparative Neurology* 396, 121–130. [https://doi.org/10.1002/\(sici\)1096-9861\(19980622\)396:1<121::aid-cne9>3.0.co;2-2](https://doi.org/10.1002/(sici)1096-9861(19980622)396:1<121::aid-cne9>3.0.co;2-2).
- Balaram, P., and J. H. Kaas. 2014. "Towards a Unified Scheme of Cortical Lamination for Primary Visual Cortex Across Primates: Insights From NeuN and VGLUT2 Immunoreactivity." *Frontiers in Neuroanatomy* 8, 81. <https://doi.org/10.3389/fnana.2014.00081>.
- Balaram, P., T. A. Hackett, and J. H. Kaas. 2013. "Differential Expression of Vesicular Glutamate Transporters 1 and 2 May Identify Distinct Modes of Glutamatergic Transmission in the Macaque Visual System." *Journal of Chemical Neuroanatomy* 50–51, 21–38. <https://doi.org/10.1016/j.jchemneu.2013.02.007>.
- Balaram, P., M. Isaamullah, H. M. Petry, M. E. Bickford, and J. H. Kaas. 2015. "Distributions of Vesicular Glutamate Transporters 1 and 2 in the Visual System of Tree Shrews (*Tupaia belangeri*)." *Journal of Comparative Neurology* 523, 1792–1808. <https://doi.org/10.1002/cne.23727>.
- Barron, A. B., and F. Mourmourakis. 2024. "The Relationship Between Cognition and Brain Size or Neuron Number." *Brain, Behavior and Evolution* 99, 109–122. <https://doi.org/10.1159/000532013>.
- Barton, R. A. 1998. "Visual Specialization and Brain Evolution in Primates." *Proceedings: Biological Sciences* 265, 1933–1937. <https://doi.org/10.1098/rspb.1998.0523>.
- Bertelsen, M. F. 2018. "Issues Surrounding Surplus Animals in Zoos." In *Fowler's Zoo and Wild Animal Medicine, Current Therapy*, edited by R. E. Miller, N. Lamberski, and P. Calle, Vol. 9, 134–137. Amsterdam, The Netherlands: Elsevier.
- Brodmann, K. 1909. *Vergleichende Lokalisationslehre der Grosshirnrinde in ihren Prinzipien dargestellt auf Grund des Zellenbaues*. Leipzig: Verlag von Johann Ambrosius Barth.
- Bryant, K. L., C. Suwyn, K. M. Reding, J. F. Smiley, T. A. Hackett, and T. M. Preuss. 2012. "Evidence for Ape and Human Specializations in Geniculostriate Projections From VGLUT2 Immunohistochemistry." *Brain, Behavior and Evolution* 80, 210–221. <https://doi.org/10.1159/000341135>.
- Butti, C., R. E. Fordyce, M. A. Raghanti, et al. 2014. "The Cerebral Cortex of the Pygmy Hippopotamus, *Hexaprotodon liberiensis* (Cetartiodactyla, Hippopotamidae): MRI, Cytoarchitecture, and Neuronal Morphology." *Anatomical Record* 297, 670–700. <https://doi.org/10.1002/ar.22875>.
- Cave, A. J. E., and D. B. Allbrook. 1959. "The Skin and Nuchal Eminence of the White Rhinoceros." *Proceedings of the Zoological Society of London* 132, 99–107.
- Celio, M. R. 1990. "Calbindin D-28k and Parvalbumin in the Rat Nervous System." *Neuroscience* 35, 375–475. [https://doi.org/10.1016/0306-4522\(90\)90091-h](https://doi.org/10.1016/0306-4522(90)90091-h).
- Clark, E. A., M. Rutlin, L. S. Capano, et al. 2020. "Cortical ROR β Is Required for Layer 4 Transcriptional Identity and Barrel Integrity." *Elife* 9, e52370. <https://doi.org/10.7554/eLife.52370>.
- Conel, J. L. 1951. *The Postnatal Development of the Human Cerebral Cortex. IV. The Cortex of the Six-Month Infant*. Cambridge, MA: Harvard University Press.
- Croner, L. J., and E. Kaplan. 1995. "Receptive Fields of P and M Ganglion Cells Across the Primate Retina." *Vision Research* 35, 7–24. [https://doi.org/10.1016/0042-6989\(94\)E0066-T](https://doi.org/10.1016/0042-6989(94)E0066-T).
- D'Arcy, C., and C. Kiel. 2021. "Cell Adhesion Molecules in Normal Skin and Melanoma." *Biomolecules* 11, 1213. <https://doi.org/10.3390/biom11081213>.
- del Campo, H. M., K. Measor, and K. A. Razak. 2014. "Parvalbumin and Calbindin Expression in Parallel Thalamocortical Pathways in a Gleaning Bat, *Antrozous pallidus*." *Journal of Comparative Neurology* 522, 2431–2455. <https://doi.org/10.1002/cne.23541>.
- Dell, L.-A., J.-L. Kruger, A. Bhagwandin, N. E. Jillani, J. D. Pettigrew, and P. R. Manger. 2010. "Nuclear Organization of Cholinergic, Putative Catecholaminergic and Serotonergic Systems in the Brains of Two Megachiropteran Species." *Journal of Chemical Neuroanatomy* 40, 177–195. <https://doi.org/10.1016/j.jchemneu.2010.05.008>.
- Douglas, R. J., and K. A. C. Martin. 2004. "Neuronal Circuits of the Neocortex." *Annual Review of Neuroscience* 27, 419–451. <https://doi.org/10.1146/annurev.neuro.27.070203.144152>.
- Elston, G. N., R. Benavides-Piccione, A. Elston, et al. 2006. "Specializations of the Granular Prefrontal Cortex of Primates: Implications for Cognitive Processing." *Anatomical Record Part A* 288A, 26–35. <https://doi.org/10.1002/ar.a.20278>.
- Elston, G. N., and P. Manger. 2014. "Pyramidal Cells in V1 of African Rodents Are Bigger, More Branched and More Spiny Than Those in Primates." *Frontiers in Neuroanatomy* 8, 4. <https://doi.org/10.3389/fnana.2014.00004>.
- Fleckman, P., and S. Brumbaugh. 2002. "Absence of the Granular Layer and Keratohyalin Define a Morphologically Distinct Subset of Individuals With Ichthyosis Vulgaris." *Experimental Dermatology* 11, 327–336. <https://doi.org/10.1034/j.1600-0625.2002.110406.x>.
- Foffani, G., J. K. Chapin, and K. A. Moxon. 2008. "Computational Role of Large Receptive Fields in the Primary Somatosensory Cortex." *Journal of Neurophysiology* 100, 268–280. <https://doi.org/10.1152/jn.01015.2007>.
- Furutani, R. 2008. "Laminar and Cytoarchitectonic Features of the Cerebral Cortex in the Risso's Dolphin (*Grampus griseus*), Striped Dolphin (*Stenella coeruleoalba*), and Bottlenose Dolphin (*Tursiops truncatus*)." *Journal of Anatomy* 213, 241–248. <https://doi.org/10.1111/j.1469-7580.2008.00936.x>.
- Gallyas, F. 1979. "Silver Staining of Myelin by Means of Physical Development." *Neurological Research* 1, 203–209. <https://doi.org/10.1080/01616412.1979.11739553>.
- García-Cabezas, M. Á., and H. Barbas. 2014. "Area 4 Has Layer IV in Adult Primates." *European Journal of Neuroscience* 39, 1824–1834. <https://doi.org/10.1111/ejn.12585>.
- Garey, L. J., and G. Leuba. 1986. "A Quantitative Study of Neuronal and Glial Numerical Density in the Visual Cortex of the Bottlenose Dolphin: Evidence for a Specialized Subarea and Changes With Age." *Journal of Comparative Neurology* 247, 491–496. <https://doi.org/10.1002/cne.902470408>.
- Geyer, S., M. Matelli, G. Luppino, and K. Zilles. 2000. "Functional Neuroanatomy of the Primate Isocortical Motor System." *Anatomy and Embryology* 202, 443–474. <https://doi.org/10.1007/s004290000127>.
- Gilbert, C. D., and T. N. Wiesel. 1979. "Morphology and Intracortical Projections of Functionally Characterised Neurones in the Cat Visual Cortex." *Nature* 280, 120–125. <https://doi.org/10.1038/280120a0>.

- Glezer, I. I., M. S. Jacobs, and P. J. Morgane. 1988. "Implications of the 'Initial Brain' Concept for Brain Evolution in Cetacea." *Behavioral and Brain Sciences* 11, 75–116. <https://doi.org/10.1017/s0140525x0005281x>.
- Glezer, I. I., P. R. Hof, and P. J. Morgane. 1998. "Comparative Analysis of Calcium-Binding Protein-Immunoreactive Neuronal Populations in the Auditory and Visual Systems of the Bottlenose Dolphin (*Tursiops truncatus*) and the Macaque Monkey (*Macaca fascicularis*)." *Journal of Chemical Neuroanatomy* 15, 203–237. [https://doi.org/10.1016/S0891-0618\(98\)00022-2](https://doi.org/10.1016/S0891-0618(98)00022-2).
- Goldstein, M. E., L. A. Sternberger, and N. H. Sternberger. 1987. "Varying Degrees of Phosphorylation Determine Microheterogeneity of the Heavy Neurofilament Polypeptide (NF-H)." *Journal of Neuroimmunology* 14, 135–148. [https://doi.org/10.1016/0165-5728\(87\)90048-8](https://doi.org/10.1016/0165-5728(87)90048-8).
- Graïc, J.-M., A. Peruffo, L. Corain, L. Finos, E. Grisan, and B. Cozzi. 2022. "The Primary Visual Cortex of Cetartiodactyls: Organization, Cytoarchitecture and Comparison With Perissodactyls and Primates." *Brain Structure and Function* 227, 1195–1225. <https://doi.org/10.1007/s00429-021-02392-8>.
- Graïc, J.-M., L. Corain, L. Finos, et al. 2024. "Age-Related Changes in the Primary Auditory Cortex of Newborn, Adults and Aging Bottlenose Dolphins (*Tursiops truncatus*) Are Located in Upper Cortical Layers." *Frontiers in Neuroanatomy* 17, 1330384. <https://doi.org/10.3389/fnana.2023.1330385>.
- Graziano, A., X. B. Liu, K. D. Murray, and E. G. Jones. 2008. "Vesicular Glutamate Transporters Define Two Sets of Glutamatergic Afferents to the Somatosensory Thalamus and Two Thalamocortical Projections in the Mouse." *Journal of Comparative Neurology* 507, 1258–1276. <https://doi.org/10.1002/cne.21592>.
- Griffen, T. C., and A. Maffei. 2014. "GABAergic Synapses: Their Plasticity and Role in Sensory Cortex." *Frontiers in Cellular Neuroscience* 8, 91. <https://doi.org/10.3389/fncel.2014.00091>.
- Griffin, G. D., S. L. Ferri-Kolwicz, B. A. S. Reyes, E. J. van Bockstaele, and L. M. Flanagan-Cato. 2010. "Ovarian Hormone-Induced Reorganization of Oxytocin-Labeled Dendrites and Synapses Lateral to the Hypothalamic Ventromedial Nucleus in Female Rats." *Journal of Comparative Neurology* 518, 4531–4545. <https://doi.org/10.1002/cne.22470>.
- Hackett, T. A., and L. A. de la Mothe. 2009. "Regional and Laminar Distribution of the Vesicular Glutamate Transporter, VGLUT2, in the Macaque Monkey Auditory Cortex." *Journal of Chemical Neuroanatomy* 38, 106–116. <https://doi.org/10.1016/j.jchemneu.2009.05.002>.
- Hakeem, A. Y., C. C. Sherwood, C. J. Bonar, C. Butti, P. R. Hof, and J. M. Allman. 2009. "Von Economo Neurons in the Elephant Brain." *Anatomical Record* 292, 242–248. <https://doi.org/10.1002/ar.20829>.
- Hashimoto, O., H. Ohtsuki, T. Kakizaki, et al. 2015. "Brown Adipose Tissue in Cetacean Blubber." *PLoS ONE* 10, e0116734. <https://doi.org/10.1371/journal.pone.0116734>.
- Imam, A., A. Bhagwandin, M. S. Ajao, and P. R. Manger. 2022. "The Brain of the Tree Pangolin (*Manis tricuspis*). IX. The Pallial Telencephalon." *Journal of Comparative Neurology* 530, 2645–2691. <https://doi.org/10.1002/cne.25349>.
- Jacobs, B., J. Lubs, M. Hannan, et al. 2011. "Neuronal Morphology in the African Elephant (*Loxodonta africana*) Neocortex." *Brain Structure and Function* 215, 273–298. <https://doi.org/10.1007/s00429-010-0288-3>.
- Jacobs, B., T. Harland, D. Kennedy, et al. 2015. "The Neocortex of Cetartiodactyls. II. Neuronal Morphology of the Visual and Motor Cortices in the Giraffe (*Giraffa camelopardalis*)." *Brain Structure and Function* 220, 2851–2872. <https://doi.org/10.1007/s00429-014-0830-9>.
- Jacobs, B., M. E. Garcia, N. B. Shea-Shumsky, et al. 2017. "Comparative Morphology of Gigantopyramidal Neurons in Primary Motor Cortex Across Mammals." *Journal of Comparative Neurology* 526, 496–536. <https://doi.org/10.1002/cne.24349>.
- Jameson, C., K. A. Boulton, N. Silove, R. Nanan, and A. J. Guastella. 2023. "Ectodermal Origins of the Skin-Brain Axis: A Novel Model for the Developing Brain, Inflammation, and Neurodevelopmental Conditions." *Molecular Psychiatry* 28, 108–117. <https://doi.org/10.1038/s41380-022-1829-8>.
- Jones, E. G. 1998. "Viewpoint: The Core and Matrix of Thalamic Organization." *Neuroscience* 85, 331–345. [https://doi.org/10.1016/s0306-4522\(97\)00581-2](https://doi.org/10.1016/s0306-4522(97)00581-2).
- Jones, E. G. 2001. "The Thalamic Matrix and Thalamocortical Synchrony." *Trends in Neuroscience* 24, 595–601. [https://doi.org/10.1016/s0166-2236\(00\)01922-6](https://doi.org/10.1016/s0166-2236(00)01922-6).
- Jones, E. G. 2003. "Chemically Defined Parallel Pathways in the Monkey Auditory System." *Annals of the New York Academy of Sciences* 999, 218–233. <https://doi.org/10.1196/annals.1284.033>.
- Jones, E. G. 2007. *The Thalamus*, 2nd Edition. Cambridge UK: Cambridge University Press.
- Kaneko, T. 2013. "Local Connections of Excitatory Neurons in Motor-Associated Cortical Areas of the Rat." *Frontiers in Neural Circuits* 7, 75. <https://doi.org/10.3389/fncir.2013.00075>.
- Kaneko, T., F. Fujiyama, and H. Hioki. 2002. "Immunohistochemical Localization of Candidates for Vesicular Glutamate Transporters in the Rat Brain." *Journal of Comparative Neurology* 444, 39–62. <https://doi.org/10.1002/cne.10129>.
- Kaplan, E., and R. M. Shapely. 1986. "The Primate Retina Contains Two Types of Ganglion Cells, With High and Low Contrast Sensitivity." *Proceedings of the National Academy of Science USA* 83, 2755–2757. <https://doi.org/10.1073/pnas.83.8.2755>.
- Killackey, H. P., and F. F. Ebner. 1972. "Two Different Types of Thalamocortical Projections to a Single Cortical Area in Mammals." *Brain, Behavior and Evolution* 6, 141–169. <https://doi.org/10.1159/00012373>.
- Kuramoto, E., T. Furuta, K. C. Nakamura, T. Unzai, H. Hoiki, and T. Kaneko. 2009. "Two Types of Thalamocortical Projections From the Motor Thalamic Nuclei of the Rat: A Single Neuron-Tracing Study Using Viral Vectors." *Cerebral Cortex* 19, 2065–2077. <https://doi.org/10.1093/cercor/bhn231>.
- Lee, B. B., P. R. Martin, and U. Grünert. 2010. "Retinal Connectivity and Primate Vision." *Progress in Retinal and Eye Research* 29, 622–639. <https://doi.org/10.1016/j.preteyeres.2010.08.004>.
- Luck, C. P., and P. G. Wright. 1964. "Aspects of the Anatomy and Physiology of the Skin of the Hippopotamus (*H. amphibius*)." *Quarterly Journal of Experimental Physiology and Cognate Medical Sciences* XLIX, 1–14.
- Lyon, D. C., N. Jain, and J. H. Kaas. 1998. "Cortical Connections of Striate and Extrastriate Visual Areas in Tree Shrews." *Journal of Comparative Neurology* 401, 109–128. [https://doi.org/10.1002/\(sici\)1096-9861\(19981109\)401:1<109::aid-cne7>3.0.co;2-i](https://doi.org/10.1002/(sici)1096-9861(19981109)401:1<109::aid-cne7>3.0.co;2-i).
- Major, H. C. 1879. "Observations on the Structure of the Brain of the White Whale (*Delphinapterus leucas*)." *Journal of Anatomy and Physiology* 13, 127–138.
- Manger, P. R. 2006. "An Examination of Cetacean Brain Structure With a Novel Hypothesis Correlating Thermogenesis to the Evolution of a Big Brain." *Biological Reviews of the Cambridge Philosophical Society* 81, 293–338. <https://doi.org/10.1017/S1464793106007019>.
- Manger, P. R., P. Pillay, B. C. Maseko, et al. 2009. "Acquisition of Brains From the African elephant (*Loxodonta africana*): Perfusion-Fixation and Dissection." *Journal of Neuroscience Methods* 179, 16–21. <https://doi.org/10.1016/j.jneumeth.2009.01.001>.
- Marin-Padilla, M. 1970. "Prenatal and Early Postnatal Ontogenesis of the Human Motor Cortex: A Golgi Study. I. The Sequential Development of the Cortical Layers." *Brain Research* 23, 167–183. [https://doi.org/10.1016/0006-8993\(70\)90037-5](https://doi.org/10.1016/0006-8993(70)90037-5).
- Marion, R., K. Li, G. Purushothaman, Y. G. Jiang, and V. A. Casagrande. 2013. "Morphological and Neurochemical Comparisons Between Pulvinar and V1 Projections to V2." *Journal of Comparative Neurology* 521, 813–832. <https://doi.org/10.1002/cne.23203>.

- Martins, A. F., N. C. Bennett, S. Clavel, et al. 2018. "Locally-Curved Geometry Generates Bending Cracks in the African Elephant Skin." *Nature Communications* 9, 3865. <https://doi.org/10.1038/s41467-018-06257-3>.
- Meyer, G., T. H. González-Hernández, and R. Ferres-Torres. 1989. "The Spiny Stellate Neurons in Layer IV of the Human Auditory Cortex. A Golgi Study." *Neuroscience* 33, 489–498. [https://doi.org/10.1016/0306-4522\(89\)90401-6](https://doi.org/10.1016/0306-4522(89)90401-6).
- Moss, C. F., and S. R. Sinha. 2003. "Neurobiology of Echolocation in Bats." *Current Opinion in Neurobiology* 13, 751–758. <https://doi.org/10.1016/j.conb.2003.10.016>.
- Murie, J. 1871. "On the Malayan Tapir, *Rhinchoerus sumatranus* (Gray)." *Journal of Anatomy and Physiology* 6, 131–512.
- Nahmani, M., and A. Erisir. 2005. "VGluT2 Immunohistochemistry Identifies Thalamocortical Terminals in Layer 4 of Adult and Developing Visual Cortex." *Journal of Comparative Neurology* 484, 458–473. <https://doi.org/10.1002/cne.20505>.
- Nassi, J. J., and E. M. Callaway. 2009. "Parallel Processing Strategies of the Primate Visual System." *Nature Reviews Neuroscience* 10, 360–372. <https://doi.org/10.1038/nrn2619>.
- Ohno, S., E. Kuramoto, T. Furuta, et al. 2012. "A Morphological Analysis of Thalamocortical Axon Fibers of Rat Posterior Thalamic Nuclei: A Single Neuron Tracing Study With Viral Vectors." *Cerebral Cortex* 22, 2840–2857. <https://doi.org/10.1093/cercor/bhr356>.
- Oishi, K., N. Nakagawa, K. Tachikawa, et al. 2016. "Identity of Neocortical Layer 4 Neurons Is Specified Through Correct Positioning Into the Cortex." *Elife* 5, e10907. <https://doi.org/10.7554/eLife.10907>.
- Pettigrew, J. D. 1986. "Flying Primates? Megabats Have the Advanced Pathway From Eye to Midbrain." *Science* 231, 1304–1306. <https://doi.org/10.1126/science.3945827>.
- Pettigrew, J. D., B. G. M. Jamieson, S. K. Robson, L. S. Hall, K. I. McNally, and H. M. Cooper. 1989. "Phylogenetic Relations Between Microbats, Megabats and Primates (Mammalia: Chiroptera and Primates)." *Philosophical Transaction of the Royal Society of London B* 325, 489–559. <https://doi.org/10.1098/rstb.1989.0102>.
- Plachocki, J. H., S. Ruiz, J. R. Rodrigues-Sosa, and M. I. Hall. 2017. "Histological Study of White Rhinoceros Integument." *PLoS ONE* 12, e0176327. <https://doi.org/10.1371/journal.pone.0176327>.
- Price, S. A., O. R. P. Bininda-Emonds, and J. L. Gittleman. 2005. "A Complete Phylogeny of the Whales, Dolphins and Even-Toed Hoofed Mammals (Cetartiodactyla)." *Biological Reviews of the Cambridge Philosophical Society* 80, 445–473. <https://doi.org/10.1017/S1464793105006743>.
- Revishchin, A. V., and L. J. Garey. 1991. "Laminar Distribution of Cytochrome Oxidase Staining in Cetacean Isocortex." *Brain, Behavior and Evolution* 37, 355–367. <https://doi.org/10.1159/000114370>.
- Rodríguez-Moreno, J., C. Porrero, A. Rollenhagen, et al. 2020. "Area-Specific Synapse Structure in Branched Posterior Nucleus Axons Reveals a New Level of Complexity in Thalamocortical Networks." *The Journal of Neuroscience* 40, 2663–2679. <https://doi.org/10.1523/JNEUROSCI.2886-19.2020>.
- Rosa, M. G. P. 1999. "Topographic Organization of Extrastriate Areas in the Flying Fox: Implications for the Evolution of Mammalian Visual Cortex." *Journal of Comparative Neurology* 411, 503–523. [https://doi.org/10.1002/\(sici\)1096-9861\(19990830\)411:3<503::aid-cne12>3.0.co;2-6](https://doi.org/10.1002/(sici)1096-9861(19990830)411:3<503::aid-cne12>3.0.co;2-6).
- Rubio-Garrido, P., F. Perez-De-Manzo, and F. Clasca. 2007. "Calcium-Binding Proteins as Markers of Layer-I Projecting vs. Deep Layer-Projecting Thalamocortical Neurons: A Double-Labeling Analysis in the Rat." *Neuroscience* 149, 242–250. <https://doi.org/10.1016/j.neuroscience.2007.07.036>.
- Schuman, B., S. Dellal, A. Prönnke, R. Machold, and B. Rudy. 2021. "Neocortical Layer I: An Elegant Solution to Top-Down and Bottom-Up Integration." *Annual Review of Neuroscience* 44, 221–252. <https://doi.org/10.1146/annurev-neuro-100520-012117>.
- Schwaller, B., I. Durussel, D. Jermann, B. Herrmann, and J. A. Cox. 1997. "Comparison of the Ca²⁺-Binding Properties of Human Recombinant Calretinin-22k and Calretinin." *Journal of Biological Chemistry* 272, 29633–29671.
- Shermann, S. M., and R. W. Guillery. 2002. "The Role of the Thalamus in the Flow of Information to the Cortex." *Philosophical Transactions of the Royal Society B Biological Sciences* 357, 1695–1708. <https://doi.org/10.1098/rstb.2002.1161>.
- Simmons, N. B. 1994. "The Case for Chiropteran Monophyly." *American Museum Novitates* 3103, 1–54.
- Skoglund, T. S., R. Pascher, and C.-H. Berthold. 1997. "The Existence of a Layer IV in the Rat Motor Cortex." *Cerebral Cortex* 7, 178–180. <https://doi.org/10.1093/cercor/7.2.178>.
- Smith, F. 1890. "Histology of the Skin of the Elephant." *Journal of Anatomy and Physiology* 24, 493–503.
- Springer, M. S., C. F. Guerrero-Juarez, M. Huelsmann, et al. 2021. "Genomic and Anatomical Comparisons of Skin Support Independent Adaptation to Life in Water by Cetaceans and Hippos." *Current Biology* 31, 2124–2139. <https://doi.org/10.1016/j.cub.2021.02.057>.
- Sternberger, L. 1986. *Immunocytochemistry*. New York: John Wiley & Sons.
- Sternberger, L. A., and N. H. Sternberger. 1983. "Monoclonal Antibodies Distinguish Phosphorylated and Nonphosphorylated Forms of Neurofilaments *In Situ*." *Proceedings of the National Academy of Science USA* 80, 6126–6130. <https://doi.org/10.1073/pnas.80.19.6126>.
- Sur, M., P. E. Garraghty, and C. J. Bruce. 1985. "Somatosensory Cortex in Macaque Monkeys: Laminar Differences in Receptive Field Size in Areas 3b and 1." *Brain Research* 342, 391–395. [https://doi.org/10.1016/0006-8993\(85\)91144-8](https://doi.org/10.1016/0006-8993(85)91144-8).
- Swanson, L. W. 2011. "The Motor System: Coordinating External and Internal Behaviors." In *Brain architecture: Understanding the Basic Plan*, edited by L. W. Swanson, 2nd Edition, 135–181. Oxford: Oxford University Press.
- Travis, F. 2012. "Core and Matrix Thalamic Nuclei: Parallel Circuits Involved in Content of Experience and General Wakefulness." *NeuroQuantology* 10, 144–149. <https://doi.org/10.14704/nq.2012.10.2.547>.
- Tsagkogeorga, G., J. Parker, E. Stupka, J. A. Cotton, and S. J. Rossiter. 2013. "Phylogenomic Analyses Elucidate the Evolutionary Relationships of Bats." *Current Biology* 23, 2262–2267. <https://doi.org/10.1016/j.cub.2013.09.014>.
- van Essen, D. C., and C. H. Anderson. 1995. "Information Processing Strategies and Pathways in the Primate Visual System." In *An Introduction to Neural and Electronic Networks*, edited by S. F. Zornetzer, T. M. McKennam, C. Lau, and J. L. Davis, 2nd Edition, 45–76. Cambridge, MA: Academic Press.
- Voelker, C. C. J., N. Garin, J. S. H. Taylor, B. H. Gähwiler, J.-P. Hornung, and Z. Molnár. 2004. "Selective Neurofilament (SMI-32, FNP-7 and N200) Expression in Subpopulation of Layer V Pyramidal Neurons *In Vivo* and *In Vitro*." *Cerebral Cortex* 14, 1276–1286. <https://doi.org/10.1093/cercor/bbh089>.
- Wong, P. Y., and J. H. Kaas. 2008. "Architectonic Subdivisions of Neocortex in the Grey Squirrel (*Sciurus carolinensis*)." *Anatomical Record* 291, 1301–1333. <https://doi.org/10.1002/ar.20758>.
- Wong, P. Y., and J. H. Kaas. 2009. "An Architectonic Study of the Neocortex of the Short-Tailed Opossum (*Monodelphis domestica*)." *Brain, Behavior and Evolution* 73, 206–228. <https://doi.org/10.1159/000225381>.
- Wong, P., O. A. Gharbawie, L. E. Luethke, and J. H. Kaas. 2008. "Thalamic Connections of Architectonic Subdivisions of Temporal Cortex in Grey Squirrels (*Sciurus carolinensis*)." *Journal of Comparative Neurology* 510, 440–461. <https://doi.org/10.1002/cne.21805>.
- Yamawaki, N., K. Borges, B. A. Suter, K. D. Harris, and G. M. G. Shepherd. 2014. "A Genuine Layer 4 in Motor Cortex With Prototypical Synaptic Circuit Connectivity." *Elife* 3, e05422. <https://doi.org/10.7554/eLife.05422>.